Breaking a Dogma: Acute Anti-Inflammatory Treatment Alters Both Post-Lesional Functional Recovery and Endogenous Adaptive Plasticity Mechanisms in a Rodent Model of Acute Peripheral Vestibulopathy.

Nada El Mahmoudi
Aix-Marseille-University: Aix-Marseille Universite https://orcid.org/0000-0001-5038-5189
Guillaume Rastoldo
Aix-Marseille-University: Aix-Marseille Universite
Emna Marouane
Aix-Marseille Université: Aix-Marseille Universite
David Péricat
Centre National de la Recherche Scientifique
Isabelle Watabe
Centre National de la Recherche Scientifique
Alain Tonetto
Aix-Marseille-University: Aix-Marseille Universite
Charlotte Hautefort
Hopital Lariboisiere Service de Neurologie
Christian Chabbert
Centre National de la Recherche Scientifique
Francesca Sargolini
Aix-Marseille Université: Aix-Marseille Universite
Brahim Tighilet (brahim.tighilet@univ-amu.fr)
Aix-Marseille-University: Aix-Marseille Universite

Research

Keywords: vestibular compensation, inflammation, corticosteroids, acute peripheral vestibulopathies.

Posted Date: March 18th, 2021

DOI: https://doi.org/10.21203/rs.3.rs-307454/v1

Version of Record: A version of this preprint was published at Journal of Neuroinflammation on August 21st, 2021. See the published version at https://doi.org/10.1186/s12974-021-02222-y.

Breaking a dogma: acute anti-inflammatory treatment alters both post-lesional functional recovery and endogenous adaptive plasticity mechanisms in a rodent model of acute peripheral vestibulopathy.

Nada El Mahmoudi[1,], Guillaume Rastoldo[1], Emna Marouane[1], David Péricat[2], Isabelle Watabe[1], Alain Tonetto[3], Charlotte Hautefort[4], Christian Chabbert[1], Francesca Sargolini[1], Brahim Tighilet[1*].

1- Aix Marseille Université-CNRS, Laboratoire de Neurosciences Cognitives, LNC UMR 7291 ; Aix-Marseille Université CNRS; Centre Saint-Charles, Case C; 3 Place Victor Hugo 13331 Marseille cedex 03, France.

2- Université de Toulouse Paul Sabatier -CNRS, Institut de pharmacologie et de biologie structurale, Toulouse, France.

3- Fédération de Recherche Sciences Chimiques Marseille FR 1739, Pôle PRATIM, 13331 Marseille Cedex 03, France

4- Department of Head and Neck Surgery, Lariboisière University Hospital, Paris, France.

*Correspondence to: Brahim Tighilet,

Phone: +33413550881; Fax: +33413550869;

Email: brahim.tighilet@univ-amu.fr

Abstract

Background: Due to their anti-inflammatory action, corticosteroids are the reference treatment for brain injuries and many inflammatory diseases. However, the benefits of acute corticotherapy are now being questioned, particularly in the case of acute peripheral vestibulopathies (APV), characterized by a vestibular syndrome composed of sustained spinning vertigo, spontaneous ocular nystagmus and oscillopsia, perceptual-cognitive, posturo-locomotor, and vegetative disorders. We assessed the effectiveness of acute corticotherapy, and the functional role of acute inflammation observed after sudden unilateral vestibular loss.

Methods: We used the rodent model of unilateral vestibular neurectomy, mimicking the syndrome observed in patients with APV. We treated the animals during the acute phase of the vestibular syndrome, either with placebo or methylprednisolone, an anti-inflammatory corticosteroid. We used both cellular and behavioral approaches with 2-way ANOVA statistical analysis to evaluate the consequences of an acute anti-inflammatory treatment on post-lesional plasticity and functional recovery.

Results: We show here, for the first time, that acute anti-inflammatory treatment alters the expression of the adaptive plasticity mechanisms in the deafferented vestibular nuclei and generates enhanced and prolonged vestibular and postural deficits.

Conclusions: These results strongly suggest a beneficial role for acute endogenous neuroinflammation in vestibular compensation. They open the way to a change in dogma for the treatment and therapeutic management of vestibular patients.

Keywords: vestibular compensation; inflammation; corticosteroids; acute peripheral vestibulopathies.

1. Introduction

Neuroinflammation is a cellular and molecular complex process, supporting the brain's response to various aggressions such as injury, infection or stress. In the central nervous system (CNS), it systematically involves microglial cells, resident brain macrophages, and astrocytes. Two types of inflammatory states must be distinguished, based on the intensity and duration of the insult. Acute neuroinflammation is the brain's immediate response. As a transient, self-regulated reaction, it is thought to play a neuroprotective role by facilitating tissue repair and post-lesional recovery. Conversely, chronic inflammation is a self-propagating and long-lasting reaction (Cherry et al., 2014) caused by a persistent stress (Streit et al., 2004), or dysregulations of the acute inflammatory resolution process (Sochocka et al., 2017). Chronic inflammation has deleterious consequences leading to neurodegeneration and is associated with CNS disorders.

The harmful impact of chronic inflammation on brain tissues have led to the administration of anti-inflammatory compounds in patients from the acute phase. Due to their anti-inflammatory action, corticosteroids have been the reference treatment for brain injuries and many inflammatory diseases for many years (Bracken et al., 1984; Fehlings et al., 2014; Hurlbert, 2000; Paragliola et al., 2017). However, the benefits of this treatment are now questioned since it does not appear to improve patients' recovery (Hurlbert, 2000; Russo and McGavern, 2016).

This is also the case for patients suffering acute peripheral vestibulopathies (APV). APV is characterized by violent, debilitating rotatory vertigo, nystagmus and cyclotorsion, during the acute phase (Strupp et al., 2019; Strupp and Brandt, 2009a), along with various perceptual-cognitive, vegetative and posturo-locomotor disorders constituting the so-called vestibular syndrome (Bronstein and Dieterich, 2019; Uffer

and Hegemann, 2016). Although the underlying cause has not yet been identified, the involvement of an inflammatory process has recently been proposed (Kassner et al., 2011), consistent with the standard corticosteroid treatment (Strupp et al., 2013; Strupp and Brandt, 2009b; Walker, 2009). However, it was recently shown that this therapeutic protocol does not significantly improve patients' functional recovery (Bronstein and Dieterich, 2019; Fishman et al., 2011; Goudakos et al., 2010; Shupak et al., 2008; Yoo et al., 2017). This suggests that the acute neuroinflammation process may play an important role in vestibular post-lesional recovery.

Among all unilateral vestibular deafferentation (UVD) models to study AVP, we focused on unilateral vestibular neurectomy (UVN), consisting in the section of one of the two vestibular nerves (Lacour and Xerri, 1980; Li et al., 1995; Péricat et al., 2017; Simon et al., 2020). UVN reproduces the human vestibular syndrome, which is thought to originate from an electrophysiological asymmetry between the ipsi- (weak activity) and contra-lesional (strong activity) vestibular nuclei (VNs) (Dutia, 2010; Mccabe and Ryu, 1969; Precht et al., 1966). With time, the progressive and spontaneous restoration of the electrophysiological balance between the ipsi- and contra-lesional VNs supports the functional recovery that accompanies the disappearance of the vestibular syndrome (Darlington and Smith, 2000; Lacour and Tighilet, 2010; Smith and Curthoys, 1989). This vestibular compensation is supported by the expression of several plasticity mechanisms in the deafferented vestibular environment (**Figure 1**), such as changes in membrane excitability (Beraneck et al., 2003; Dutheil et al., 2016), release of neurotrophic factors (Dutheil et al., 2016), and reactive neurogliogenesis (Dutheil et al., 2009; Rastoldo, 2021; Tighilet et al., 2007).

UVN is also known to cause a neuroinflammatory reaction by inducing astroglial (Dutheil et al., 2011, 2009; Rastoldo et al., 2021) and microglial (Dutheil et al., 2016;

Rastoldo et al., 2021) responses, which are associated with the expression of two key inflammatory factors in the deafferented VNs : the tumor necrosis factor-alpha (TNF-alpha) and the nuclear factor-kappa B (NF-kB) (Liberge et al., 2010). UVN also activates the hypothalamo-pituitary-adrenal (HPA) axis (Tighilet et al., 2009; Saman et al., 2012) leading to a strong release of anti-inflammatory endogenous corticosteroids (EC) in the deafferented VNs (Tighilet et al., 2009), thus confirming UVN-induced neuroinflammatory process.

The aim of this study is to assess the functional role of the acute neuroinflammation process in functional recovery after UVN. To do so, we investigated the effects induced by pharmacological blockade of acute inflammation following UVN on the expression of the plasticity mechanisms observed in the deafferented VNs, as well as on the kinetics of vestibular compensation in the adult rodent.

2. Materials & Methods

2.1 Animals & Ethical statements

This study was performed on 61 adult Long Evans female rats weighing between 250 and 350 g. All experiments were performed in accordance with the National Institutes of Health's Guide for Care and Use of Laboratory Animals (NIH Publication no. 80-23) revised in 1996 for the UK Animals (Scientific Procedures) Act of 1986 and associated guidelines or the Policy on Ethics approved by the Society for Neuroscience in November 1989 and amended in November 1993 and under veterinary and National Ethical Committee supervision (French Agriculture Ministry Authorization: B13-055-25). The present study was specifically approved by Neurosciences Ethics Committee N°71 of the French National Committee of animal experimentation. Every effort was made to minimize both the number and the suffering of animals used in this

experiment. Rats had free access to food and water and were housed with a littermate in an enriched environment under a constant 12h light.

2.2 Study design

To determine the role of the acute inflammatory process in vestibular compensation, we used an anti-inflammatory compound, methylprednisolone (10mg/kg), administrated intraperitoneally (*i.p*) immediately after the UVN and during the acute phase (first 3 days (d) after the lesion). We observed the effects of this treatment at both cellular and behavioral levels (**Figure 2**). To do so, we randomly divided the animals into 3 groups: a sham group (n=21), submitted to the same surgical approach as UVN without sectioning the nerve; a UVN+placebo group (n=21), lesioned and treated with NaCl 0.9%; and a UVN+methylprednisolone (UVN+met) group (n=19), lesioned and treated with methylprednisolone. For each group, 4 animals were sacrificed at the end of the acute phase (d3) and 4 animals at the end of the behavioral study (d30) for cellular investigations. At the cellular level, we looked for changes in plasticity markers in the deafferented VNs at 3 and 30 days after the lesion. At the behavioral level, we measured the kinetics of the vestibular compensation using different behavioral assessments performed at different time points after the lesion.

2.3 Unilateral vestibular neurectomy (UVN)

We used the model of left unilateral vestibular neurectomy in the adult rat (Péricat et al., 2017) consisting in sectioning the left vestibular nerve. Animals were anesthetized with isoflurane (4%) 30 minutes after a subcutaneous injection of buprenorphine (Buprecare®; 0.02 mg/kg). The animals were intubated, and the anaesthesia was maintained during the surgery with isoflurane (3%). To access the left vestibular nerve, we used the tympanic bulla approach (see Péricat et al., 2017 for details) to access the vestibulocochlear nerve through the tympanic bulla and through the cochlea. The

left vestibular nerve was then sectioned at a post-ganglion level, close to the brainstem. For the sham group (n=22), the surgery was limited to the perforation of the tympanic bulla. Before awakening, the animals were injected subcutaneously with a solution of Ringer Lactate (Virbac; 10 ml/kg) to alleviate the dehydration resulting from the surgery. The success of the UVN (n= 44) was attested by the immediate appearance of a characteristic vestibular syndrome composed of postural, locomotor and oculomotor deficits (Péricat et al.,2017).

2.4 Pharmacological treatments

The pharmacological treatments were administrated once per day during three days after the UVN, corresponding to the acute phase of the vestibular syndrome in rodents (Péricat et al., 2017). The UVN+placebo group was administrated with NaCl 0.9% (2ml/kg) while the UVN+met group was treated with methylprednisolone (Solu-médrol®, 10mg/kg), a corticosteroid classically used in vestibular patients (Fishman et al., 2011; Goudakos et al., 2014, 2010; Strupp et al., 2013; Yoo et al., 2017).

2.5 Cellular investigations

2.5.1 Tissue preparation

The animals received an *i.p* injection of 5-Bromo-2'-deoxyuridine (BrdU: 200mg/kg) dissolved in NaCl 0.9% 3 days after the lesion and were sacrificed either at 3 (n=4 per group) or 30 days after the lesion (n=4 per group). The rats were deeply anesthetized with a mixture of ketamine (Imalgène 1000®, 60mg/kg) and medetomidine (Domitor®0.25mg/kg) for intracardiac perfusion. First, an intracardiac injection of 400ml of isotonic saline (0.9% NaCl) was performed, followed by an injection of 400ml of freshly prepared solution (4% paraformaldehyde (PFA) and in 0.1 M phosphate buffer (PB), pH 7.4). At the end of the perfusion, brains were extracted and post-fixed overnight at 4°C in PFA 4% solution. Brains were then rinsed and cryoprotected by

successive baths into sucrose solutions at increasing concentrations (10%, 20%, 30% of D-saccharose in 0.1M PB each for 24h at 4°C). Brains were then frozen with CO2 gas and cut into serial 40µm frontal sections with a cryostat (Leica) for immunochemistry.

2.5.2 Immunohistochemistry

Immunochemical labeling was performed according to previously validated protocols (Dutheil et al., 2016, 2013; Rastoldo et al., 2021; Tighilet et al., 2007). For BrdU immunohistochemistry, sections were incubated with a BrdU antibody (1:100, Dako, M0744). Cell proliferation was analysed by a *i.p* injection of BrdU. Animals were then sacrificed either 3 days (d3) or 30 days (d30) after the injection to assess short-term cell proliferation and long-term survival of the proliferative cells, respectively. The low doses administered to animals were enough to mark the cells in the S-phase of the cell cycle (Dutheil et al., 2011; Tighilet et al., 2007). For glucocorticoid receptor (GR) immunohistochemistry, we used a GR antibody (1:300, ThermoFisher, PA1-511A). For glial cells immunohistochemistry, we used a microglial marker, ionized calcium-binding adapter molecule 1 (IBA1) (1:2000, Wako, Cat#019-19741), and an astrocytic marker, glial fibrillary acidic protein (GFAP) (1:200, Dako, Z033401-2). For potassium–chloride cotransporter 2 (KCC2) immunohistochemistry, sections were incubated with a KCC2 antibody (1:200, Merck, 07-432). For each section, we used DAPI (1:5000, Merck, D9542) incubation to mark the nucleus. To visualize the primary antibodies, we used the following secondary antibodies for immunostaining: goat anti-rabbit conjugated with Alexa Fluor 488 (1:500, Invitrogen, A11008) and goat anti-mouse IgG conjugated with Alexa Fluor 594 (1:500, Invitrogen, A11005).

2.5.3 Cell counting methods and quantification of KCC2 immunoreactivity

198 Cell counts were performed according to previously validated protocols (Dutheil et al.,
199 2016, 2011, 2009; Rastoldo et al., 2021). All cellular investigations were performed in
200 the left VNs at 3 and 30 days after left UVN or sham surgery. The recognition,
201 localization and delimitation of the VNs of the brainstem was performed on cresyl
202 violet-stained sections based on Paxinos and Watson's stereotaxic atlas (Paxinos and
203 Watson, 2009). For quantification, 1 in 10 serial sections was used starting from the
204 beginning (-9.84 mm relative to the bregma) to the end of the VNs (-13.08 mm relative
205 to bregma (Paxinos and Watson, 2009)). Ten sequential sections of the deafferented
206 (left) VNs were assessed. Immunoreactive (ir) cells were analysed using confocal
207 imaging with a Zeiss LM 710 NLO laser scanning microscope equipped with a 63X/1.32
208 BA oil immersion lens. Numbers of IBA1-, GFAP-, GR- and BrdU- ir cells were counted
209 using an integrated microscopic counting chamber that delineated the region of interest
210 by a square of 425.10mm^2. The average cell counts from 10±2 sections were used for
211 statistical analysis. For GR quantification, we calculated the percentage of GR/DAPI
212 ir-cells among GR-ir cells to assess for GR nuclear localization. For BrdU
213 quantification, we calculated the percentage of BrdU ir-cells persisting at d30 to assess
214 the survival of the proliferative cells observed at d3.
215 The quantification of the KCC2 immunolabeling was performed according to a
216 previously published protocol (Tighilet et al., 2016) using a custom program written in
217 Matlab® (TheMathworks, Inc.). Briefly, the program allows analysis of the fluorescence
218 at the plasma membrane of neurons. The background was assessed by calculating
219 the average fluorescence in a visually selected area devoid of neurons or any other
220 stained structure. From this region, a threshold was then derived, equal to the average
221 immunofluorescence plus three times the standard deviation. All data were then
222 subtracted from this threshold and only positive values were conserved for further

analysis. A region of interest was drawn around the neuronal plasma membrane of each cell body. The program calculated the average fluorescence within the region of interest over data that were 20% above the maximum values. This thresholding insured that all pixels taken for calculating the average were part of the plasma membrane and that the same criterion was used for all slices in all conditions.

2.5.4 Cellular data statistical analysis

To avoid any bias, the cellular analysis was performed under blind conditions. For each cellular marker, the results are expressed as mean ± standard error mean (SEM). We performed a two-way ANOVA to test the impact of the post-operative time and the impact of the group on the expression of the cellular markers, followed by post hoc Tukey's multiple comparisons analysis. Results were considered significant at $p<0.05$.

2.6 Behavioral investigations

For each behavioral investigation, acquisitions were performed before the surgery (preop) and at different time-points (days) during the post-operative time (d1, d2, d3, d7, d14, d21, and d30) to assess, for each group, the intensity of the vestibular syndrome and the kinetics of the vestibular compensation.

2.6.1 Qualitative assessment of the vestibular syndrome

We assessed the intensity of the vestibular syndrome and its kinetic by using a cumulative qualitative scale listing typical postural, locomotor and oculomotor deficits classically induced by UVN. Each behavioral symptom corresponds to a score on the qualitative scale (tumbling: 5; retropulsion: 4; circling: 3; bobbing: 2; head-tilt: 1). The score corresponds to the sum of the different symptoms, reflecting the severity of the vestibular syndrome and the alteration of the vestibular function (see Péricat et al., 2017 for details).

2.6.2 Support surface measurement after Tail Suspension Test (TST)

Vestibular function plays a crucial part in postural stability and posture-related responses according to behavioral context (McCall et al., 2017). We assessed the postural stability after UVN by measuring the support surface (i.e., the area between the four paws of the animal), a well-known indicator used in various models of vestibular loss (Dutheil et al., 2016; Liberge et al., 2010; Marouane et al., 2020; Tighilet et al., 2015). To address directly the vestibular function, we realized performed the tail suspension test (TST) by holding the animal by the tail and subjecting it to vertical traction over a height of about 50 cm. Sudden vertical acceleration of the animal activates the remaining vestibular receptors, reactivating the vestibular syndrome while drastically reducing tactile and proprioceptive inputs (Cassel et al., 2018; Tighilet et al., 2017), leaving the effectiveness of the vestibulo-spinal reflex principally under the control of the vestibular function. The animals were placed in an open field and a picture was taken each time the animal landed after the TST test. The support surface was calculated in cm^2, using an image analysis system developed on Matlab®. For each animal, ten repeated measurements were taken and averaged before the operation (preop) and at each post-operative time-point starting from d3. All the measurements were normalized so that each animal acted as its own control. To do so, for each rat, we used the preop value as the baseline (referenced as 1 for each rat) and we compared each value measured during the post-operative time to the baseline to visualize the changes of the support surface.

2.6.3 Quantitative assessment of postural function

We used the second version of the dynamic weight-bearing device (DWB2®) to assess) and quantify the postural function of rats after UVN, under ecological conditions (for details see (Marouane et al., 2020; Tighilet et al., 2017). The animals

were individually placed in this device and moved freely for 5min. The apparatus allows quantification of the support forces of each part of the animal's body.

We analysed the weight distribution of the animals along the lateral axis, previously described as a significant indicator of postural balance (Marouane et al., 2020; Tighilet et al., 2017). It is represented in this study as the laterality index, corresponding to the difference in weight distributed between the right and left paws. We also used the DWB2® device to measure the rearing time (i.e., time spent on the two hind paws), considered as a significant indicator of the animal's ability to stand, reflecting its postural balance control (Tighilet et al., 2017). This apparatus enabled us to quantify a typical behaviour of a unilateral vestibular loss, ipsilesional circling, defined as fast rotations of the animal toward the lesioned side (Marouane et al., 2020; Péricat et al., 2017). The circling behaviour was assessed by counting the number of fast laps performed during an acquisition.

We also extracted posturographic parameters at the pre-operative time point and two post-operative time points: d3, corresponding to the acute phase of the vestibular syndrome, and d30, corresponding to the compensated phase of the vestibular syndrome. For the following parameters, data were normalized according to pre-operative values so that each rat acted as its own control:

- the average time spent by the animals with their abdomen on the ground sensors, during static and dynamic periods, which has been described and validated as a postural strategy during the acute phase after UVN (Marouane et al., 2020). This parameter, expressed in grams, was normalized according to pre-operative values by subtracting the pre-operative value to each post-lesional value measured during the post-operative time.

- the mean position of the barycenter which was calculated using the coordinates of each paw and their respective support forces (cf. equations (Equ) 3 and 4). The position of the barycenter was calculated at each period when the animal was stationary and on its four paws.

Equ (3) $$Barx = \frac{FLx*FLw+FRx*FRw+RLx*RLw+RRx*RRw}{FLw+FRw+RLw+RRw}$$

Equ (4) $$Bary = \frac{FLy*FLw+FRy*FRw+RLy*RLw+RRy*RRw}{FLw+FRw+RLw+RRw}$$

Based on the coordinates of the rat's barycenter over time, we were able to trace the statokinesigram for each acquisition. Statokinesigrams show the trajectories in 2D of the barycenter and the center of gravity of each paw every time the calculation is performed, when rats were static and on their four paws. An average weighted by the duration of each of these moments is then established for each acquisition.

- We extracted the mean lateral position of the barycenter (in centimeters (cm)) that we normalized according to pre-operative values by subtracting the pre-operative value from each post-operative value measured during the post-operative time.
- To analyse the stability of the barycenter, we measured its maximum lateral deviation (maximum value of *Bary* minus minimum value of *Bary)* used here as an indicator of lateral instability. We also measured barycenter inertia, a measure of the barycenter positions' dispersion during the acquisitions, reflecting postural stability. For both parameters, data were normalized as a ratio according to pre-operative values.

These acquisition methods have been recently published and validated for this rodent model of vestibulopathy by our group (Marouane et al., 2020).

2.6.4 Quantitative assessment of the posturo-locomotor activity

We assessed the posturo-locomotor activity of the animals under ecological conditions by measuring different parameters known to be affected by UVN in rats (see (Rastoldo et al., 2020) for details). At the beginning of the session, rats were placed individually in the center of an open field (80x80x40cm) for 10 minutes and tracked with Ethovision ™ XT 14 software (Noldus). We measured the total distance moved (cm), the mean velocity (cm/s) and the mean acceleration (cm/s^2) to assess the locomotor activity. These locomotor parameters were normalized by dividing each value measured during the post-operative time by the baseline (i.e., the value in the pre-operative time) to visualize the progression of the parameters. We also measured a postural variable, the mean body torsion defined as the angle between the nose and the tail of the rat during the acquisitions (expressed in degrees, positive values corresponding to torsion toward the left side and negative values to torsion toward the right side). This parameter was normalized for each rat by subtracting the baseline pre-operative value from the post-operative measures to visualize the increase or decrease of the parameter with time. These acquisition methods have been recently published and validated by our group (Rastoldo et al., 2020).

2.6.5 Behavioral statistical analysis

The results are expressed as mean + SEM. We performed a two-way repeated measures ANOVA ('group' and 'time' factors) to test the impact of the post-operative time and the impact of the group on the behavioral markers, followed by post hoc

345 analysis with Tukey's multiple comparisons test. Results were considered significant
346 at $p<0.05$.
347
348 # 3.Results
349 ## 3.1 Cellular results
350 ### 3.1.1 Acute anti-inflammatory treatment significantly reduces glial reactions in
351 ### the deafferented medial vestibular nuclei (VNs)
352 Immunohistochemistry investigation for the number of microglial cells using IBA1
353 antibody showed a significant decrease after UVN and acute anti-inflammatory
354 treatment (**Figure.3A-B**). Statistical analysis revealed a significant 'group' effect (two-
355 way ANOVA; 'group': $F(2,67)=32.3$, $p<0.001$). In the sham group, we observed a basal
356 and persistent number of IBA1-ir cells) in the medial VNs. After UVN, there was a
357 significant increase in the number of IBA1-ir cells in the deafferented medial VNs of
358 the UVN+placebo group compared to the sham group at d3 (Tukey post-hoc; $p<0.001$),
359 that persisted at d30 (Tukey post-hoc; $p<0.05$). Conversely, in the UVN+met group, no
360 significant change was observed in the number of IBA1-ir cells compared to the sham
361 group. Compared to the UVN+placebo group, the UVN+met group displayed a
362 significantly lower number of IBA1-ir cells at d3 (Tukey post-hoc; $p<0.001$) and d30
363 (Tukey post-hoc; $p<0.01$).
364 Similarly, the number of astroglial cells, visualized with GFAP-ir cells, was reduced
365 after UVN and acute anti-inflammatory treatment (**Figure.3C-D**). The statistical
366 analysis revealed significant 'group' 'group x time' effects (two-way ANOVA; 'group':
367 $F(2,63)=43.1$, $p<0.001$; 'group x time': $F(2,63)=3.77$, $p<0.05$; 'time': $F(1,63)=2.87$,
368 $p=0.09$). The quantification of the GFAP-ir cells in the sham group revealed a stable
369 and moderate number of immunoreactive cells over time. After UVN, there was a

significant increase in the number of GFAP-ir cells in the deafferented medial VNs of the UVN+placebo group compared to the sham group at d3 (Tukey post-hoc; $p<0.001$) persisting at d30 (Tukey post-hoc; $p<0.01$). As for IBA1-ir cells, we observed no significant changes in the number of GFAP-ir cells in the UVN+met group compared to the sham group. Compared with the UVN+placebo group, the UVN+met group showed a significant decrease in the number of GFAP-ir cells at d3 (Tukey post-hoc; $p<0.001$) persisting at d30 (Tukey post-hoc; $p<0.05$)

3.1.2 Acute anti-inflammatory treatment significantly reduces GR nuclear localization in the medial VNs 3 days post-UVN

Immunohistochemistry for GR nuclear localization, investigated through the percentage of GR/DAPI ir-cells, revealed a significant decrease after acute anti-inflammatory treatment during the acute phase. (**Figure.4A-B**). Statistical analysis revealed a significant 'group' effect (two-way ANOVA; 'group': $F(2,56) = 9.69$, $p<0.001$). For the sham group, the percentage of GR/DAPI ir-cells in the medial VNs was stable over time. After UVN and placebo treatment, strong nuclear GR immunoreactivity was attested by the significant increase of GR/DAPI at d3 compared to the sham group (Tukey post-hoc; $p<0.01$), persisting at d30 (Tukey post-hoc; $p<0.05$). Conversely, we did not observe in the UVN+met group any significant differences in the number of GR/DAPI ir-cells compared to the sham group. Compared to the UVN+placebo group, the UVN+met group showed a significant decrease in the number of GR/DAPI ir-cells at d3 (Tukey post-hoc; $p<0.05$).

3.1.3 Acute anti-inflammatory treatment alters proliferation and survival of new cells in the deafferented medial VNs

Investigations for cell proliferation and survival, analysed using BrdU antibody, revealed a significant decrease of cell proliferation and survival after acute anti-inflammatory treatment (**Figure 4C-D**). Statistical analysis revealed significant 'time', 'group' and 'group x time' effects (two-way ANOVA; 'time': $F(1,45) = 6.95$, $p<0.05$; 'group': $F(2,45) = 51.3$, $p<0.001$; 'time x group': $F(2,45) = 5.48$, $p<0.01$).

In the sham group, we observed a very low rate of BrdU-ir cells. A strong and significant increase in the number of BrdU-ir cells was detected in the deafferented medial VNs for the UVN+placebo group compared to the sham group at d3 (Tukey post-hoc; $p<0.001$) and d30 (Tukey post-hoc; $p<0.001$), corresponding to 94.5% mean rate of survival. In the UVN+met group, we observed a significant increase of BrdU-ir cells at d3 compared to the sham group (Tukey post-hoc; $p<0.05$) but significantly lower compared to the UVN+placebo group (Tukey post-hoc; $p<0.05$). In addition, in the UVN+met group, we observed, at d30, a significantly lower number of BrdU-ir cells compared to the UVN+placebo group (Tukey post-hoc; $p<0.001$) corresponding to a mean survival rate of 10.34%.

3.1.4 Acute anti-inflammatory treatment hinders the change in KCC2 expression in the lateral vestibular nuclei (VNs) 3 days post UVN.

We studied changes in the expression of the cation-chloride cotransporter KCC2, the level of which at the membrane determines the action of GABA on the neuron membrane's excitability. We focused our analysis on the giant neurons of the lateral VNs as they contain excitatory glutamatergic neurons involved in vestibulo-spinal pathways. We observed a significant increase of KCC2 expression after UVN and acute anti-inflammatory treatment during the acute phase (**Figure 4E-F**). Statistical analysis of KCC2 fluorescence intensity revealed significant 'time', 'group' and 'group

x time' effects (two-way ANOVA; 'time': $F(1,177) = 19.9, p<0.001$; 'group': $F(3,177) = 59.9$, $p<0.001$; 'time x group': $F(3,177) = 17.7$, $p<0.001$). For the sham group a persistent mean of KCC2 fluorescence intensity was observed over time. A significant reduction in the mean KCC2 immunofluorescence intensity was observed in the UVN+placebo group compared to the sham group at d3 (Tukey post-hoc; $p<0.001$), no longer present 30 days after UVN. In the UVN+met group, a significant increase in the mean KCC2 fluorescence intensity was observed compared to the sham group at d3 (Tukey post-hoc; $p<0.01$) persisting at d30 (Tukey post-hoc; $p<0.05$). Compared to the UVN+placebo group, the UVN+met group displayed a significantly greater mean KCC2 fluorescence intensity at d3 (Tukey post-hoc; $p<0.001$).

3.2 Behavioral results

3.2.1 Acute anti-inflammatory treatment significantly increases the intensity of the vestibular syndrome after UVN

The intensity and time course of the vestibular syndrome were analysed using a score on a qualitative scale, listing typical posturo-locomotor symptoms induced by UVN. We observed a significantly increased vestibular syndrome after UVN and acute anti-inflammatory treatment (**Figure 5A-B**). Statistical analysis revealed significant 'time', 'group' and 'time x group'' effects (two-way repeated measures ANOVA, 'time': $F(7,322)=78.4$, $p<0.001$; 'group': $F(2,46)=72$, $p<0.001$; 'time x group': $F(14,322)=21.5$, $p<0.001$). We observed for the UVN+placebo group a characteristic kinetic pattern) (Marouane et al., 2020; Péricat et al., 2017; Tighilet et al., 2017), with an intense vestibular syndrome during the first three days after UVN, decreasing progressively over time but still significantly persistent compared to the sham at all time

points (Tukey post-hoc ; $p<0.001$ at all-times). In the UVN+met group the vestibular deficits were significantly greater compared to the UVN+placebo group at all time points from d3 (Tukey post-hoc; $p<0.05$) to d30 (Tukey post-hoc; $p<0.05$) indicating an intensified vestibular syndrome after acute anti-inflammatory treatment.

3.2.2 Acute anti-inflammatory treatment significantly increases postural instability during vestibulo-spinal reflex reactivation after UVN

To assess the postural stability after UVN, we analysed the support surface after tail suspension test (TST). In four-footed animals, vestibular syndrome leads to an increased support surface delimited by the four paw pads. This parameter provides a good estimation of postural instability after UVN since it displays the tonic asymmetry of extensor and flexor muscles of the anterior and posterior paws that results from vestibular deafferentation. In addition, this parameter is measured after TST, which enables us to appreciate the effectiveness of the vestibulo-spinal reflex under the control of vestibular function recovery. We observed a significant increase of postural instability after UVN and acute anti-inflammatory treatment (**Figure 5C**). Statistical analysis revealed significant 'time', 'group' and 'time x group' effects (two-way repeated measures ANOVA, 'time': $F(5,145)=7.46$, $p<0.001$; 'group': $F(2,29)=24.5$, $p<0.001$; 'time x group': $F(10,145)=11.1$,$p<0.001$). For the sham group, we observed a significant diminution of the support surface over time (preop versus d30; Tukey post-hoc; $p<0.05$), probably reflecting habituation to the test. Conversely, a significant increase of the support surface was observed in the UVN+placebo group compared to the sham group at d3 (Tukey post-hoc; $p<0.01$). This significant difference persisted until d21 (Tukey post-hoc; $p<0.05$) and was no longer present at d30. A significant increase of the support surface parameter was also observed in the UVN+met group

compared to the sham group from d3 (Tukey post-hoc; $p<0.001$) to d30 (Tukey post-hoc; $p<0.001$). The enlargement of the support surface was significantly more pronounced in the UVN+met group compared the UVN+placebo group from d7 (Tukey post-hoc; $p<0.001$) to d30 (Tukey post-hoc; $p<0.001$), indicating enhanced and persistent postural instability in the UVN+met group over time.

3.2.3 Effect of acute anti-inflammatory treatment on postural parameters analysed by the dynamic weight distribution device

3.2.3.1 Weight distribution along the lateral axis

To visualize the weight distribution along the lateral axis, we represented a weight laterality index corresponding to the weight distributed on the right paws minus the weight distributed on the left paws. We observed a significant increase of the weight distributed on the left paws after UVN for both UVN+placebo and UVN+met groups (**Figure 6A**). Statistical analysis revealed significant 'time', 'group' and 'time x group'' effects (two-way repeated measures ANOVA, 'time': $F(7,140)=10.8$, $p<0.001$; 'group': $F(2,20)=10.6$, $p<0.001$; 'time x group': $F(14,140)=2.39$, $p<0.01$). As previously described (Marouane et al., 2020; Tighilet et al., 2017), a significant increase of the weight distribution on the left paws was observed in the UVN+placebo group compared with the sham group at d7 (Tukey post-hoc; $p<0.05$), still present at d30 (Tukey post-hoc; $p<0.01$). In the UVN+met group, this increase appeared at d3 compared to the sham group (Tukey post-hoc; $p<0.05$) and increased over time until d30 (Tukey post-hoc; $p<0,001$).

3.2.3.3 Rearing time

The percentage of rearing time was used as an indicator of balance control, reflecting the animals' ability to stand. We observed a significant decrease of the rearing time

after UVN for both UVN+placebo and UVN+met groups (**Figure 6B**). Statistical analysis revealed significant 'time', 'group' and 'time x group' effects (two-way repeated measures ANOVA, 'time': $F(7,140) = 15.15$, $p<0.001$; 'group': $F(2,20) = 35.5$, $p<0.001$; 'time x group': $F(14,140) = 2.77$, $p<0.01$). For the sham group, we observed that the animals spent on average 50% of their time on the two hind paws. For the UVN+placebo group, we observed a significant decrease compared to the sham group at d1 (Tukey post-hoc; $p<0.001$) persisting until d14 (Tukey post-hoc; $p<0.05$). For the UVN+met group, we observed the same decrease compared to the sham group at d1 (Tukey post-hoc; $p<0.001$) persisting significantly until d30 (Tukey post-hoc; $p<0.01$). The rearing time was greater in the UVN+placebo group compared to the UVN+met group at d30 although not significantly (respectively 37.4%±3.7 versus 26.5%±5.2; Tukey post-hoc; $p=0.05$).

3.2.3.4 Left circling behaviour (ipsilesional rotations)

We quantified the number of left circling (i.e., fast rotations toward the ipsilesional side), known to arise in UVN rat model during the acute phase (Marouane et al., 2020; Péricat et al., 2017). We observed a significant increase of the left circling after UVN and acute anti-inflammatory treatment (**Figure 6C).** Statistical analysis revealed significant 'time', 'group' and 'time x group' effects (two-way repeated measures ANOVA, 'time'": $F(2,34) = 3.84$, $p<0.05$; 'group': $F(2,17) = 10$, $p<0.01$; 'time x group': $F(4,34) = 4.28$, $p<0.01$). In the UVN+placebo group, we observed that the left circling behavior was no longer present compared to the sham group, at both d3 and d30. In contrast, this behavior was significantly increased in the UVN+met group compared to the sham group at d3 (Tukey post-hoc; $p<0.001$) and d30 (Tukey post-hoc; $p<0.05$). Similar results were obtained when comparing the UVN+met and UVN+placebo groups with a significant

increase of the left circling in the UVN+met group at d3 (Tukey post-hoc; $p<0.001$) and d30 (Tukey post-hoc; $p<0.05$).

3.2.3.5 Weight distributed on the abdomen

We quantified the weight distributed on the abdomen during the acquisitions. This parameter was shown to increase during the acute phase after UVN, especially during the first day (Marouane et al.,2020), suggesting a strategy used by the animals to maintain balance with the use of a new support point to promote stability. We observed a significant increase of the weight distributed on the abdomen after UVN and acute anti-inflammatory treatment during the compensated phase (**Figure 7B**). Statistical analysis revealed significant 'group' effect (two-way repeated measures ANOVA, 'group': $F(2,17) = 10$, $p<0.01$). We observed that this postural strategy was absent in the UVN+placebo group compared to sham group at d3 and d30. In the UVN+met group, however, we observed that the animals distributed more weight on the abdomen at d30 compared to both sham (Tukey post-hoc; $p<0.001$) and UVN+placebo groups (Tukey post-hoc; $p<0.01$).

3.2.3.6 Barycenter posturographic analysis

We calculated the position of the barycenter at each moment, when the animal was stationary and on its four paws, which enabled us to trace the average positions of the paws and the position of the barycenter of each animal, represented here as statokinesigrams (**Figure 7A**). These statokinesigrams showed us different postural patterns depending on the group of rats and the post-lesion time, leading us to analyse 3 parameters representing the position and stability of the barycenter along over time.

3.2.3.6.1. Mean lateral position of the barycenter

We analysed the patterns of change of the mean lateral position of the barycenter at d3 and d30. Positive values represent a displacement of the barycenter toward the right side while negative values represent a displacement of the barycenter toward the left side. We observed a significant displacement of the barycenter toward the left side after UVN for both UVN+placebo and UVN+met groups (**Figure 7.C**). Statistical analysis revealed significant 'group' effect (two-way repeated measures ANOVA, 'group': $F(2,18) = 8.5$, $p<0.01$). In the UVN+placebo group, we observed a significant displacement of the barycenter toward the left side compared to the sham group at d30 (Tukey post-hoc; $p<0.01$). For the UVN+met group, this displacement toward the left side was significant at d3 compared to the sham group (Tukey post-hoc; $p<0.01$) and still present at d30 (Tukey post-hoc; $p<0.01$).

3.2.3.6.2 Barycenter inertia

We analysed the barycenter inertia, a measure of the barycenter position dispersion during the acquisitions, reflecting its stability. We observed a significant increase of the barycenter inertia after UVN and acute anti-inflammatory treatment during the compensated phase (**Figure 7.D**). Statistical analysis revealed significant 'group' effect (two-way repeated measures ANOVA, 'group': $F(2,19) = 5.33$, $p<0.05$). This parameter was significantly greater in the UVN+met group at d30 compared to both sham (Tukey post-hoc; $p<0.01$) and UVN+placebo groups (Tukey post-hoc; $p<0.05$).

3.2.3.6.3 Barycenter maximum lateral deviation

We analysed the stability of the barycenter along the lateral axis by calculating the barycenter maximum lateral deviation (By_{max} minus By_{min}). We observed a significant increase of the barycenter maximum lateral deviation after UVN and acute anti-

570 inflammatory treatment during the compensated phase (**Figure 7E**). Statistical
571 analysis revealed significant 'group x time' effect (two-way repeated measures
572 ANOVA, 'group x time': $F(2,17) = 5.91$, $p<0.05$). This parameter was greater in the
573 UVN+met group at d30 compared to sham (Tukey post-hoc; $p<0.05$) and
574 UVN+placebo (Tukey post-hoc; $p<0.05$) groups.
575
576 **3.2.4 Effect of acute anti-inflammatory treatment on posturo-locomotor**
577 **parameters analysed by videotracking.**
578
579 3.2.4.1 Mean body torsion of the animals
580 We measured the changes in the mean body torsion over time following UVN. This
581 parameter has previously been shown to reflect postural alteration after unilateral
582 vestibular deafferentation (UVD) (Vidal et al., 1993). Positive values represent
583 increased body torsion towards the left side (side of the vestibular lesion) and negative
584 values indicate increased body torsion towards the right side. We observed a
585 significant increase of the mean body torsion towards the left side after UVN and acute
586 anti-inflammatory treatment during the acute phase (**Figure 8A**). Statistical analysis
587 revealed significant 'time', 'group' and 'time x group'' effects (two-way repeated
588 measures ANOVA, 'time': $F(7,217) = 6.83$, $p<0.001$; 'group'': $F(2,31) = 14.5$, $p<0.001$;
589 'time x group': $F(14,217)=6$, $p<0.001$). A significant increase of the mean body torsion
590 toward the left side was observed for the UVN+placebo group compared with the sham
591 group at d1 (Tukey post-hoc; $p<0.001$), persisting at d2 (Tukey post-hoc, $p<0.05$). This
592 increase was significantly greater in the UVN+met group compared to the sham group
593 at d1 (Tukey post-hoc; $p<0.001$) and persisted until d7 (Tukey post-hoc; $p<0.05$). It

was significantly more pronounced in the UVN+met group compared to the UVN+placebo group at d1 (Tukey post-hoc; $p<0.05$) and d2 (Tukey post-hoc; $p<0.05$).

3.2.4.2 Total distance travelled

We investigated the total distance travelled in the open field. We observed a significant increase of this parameter after UVN for both UVN+placebo and UVN+met groups in the compensated phase (**Figure 8B**). Statistical analysis revealed significant 'time', 'group' and 'time x group' effects (two-way repeated measures ANOVA, 'time': $F(7,203)=61.5$, $p<0.001$; 'group': $F(2,29)=4.94$, $p<0.05$; 'time x group': $F(14,203)=21.5$, $p<0.001$). We observed that the UVN+placebo group travelled a significantly greater distance than the sham group from d14 (Tukey post-hoc; $p<0.001$) until d30 (Tukey post-hoc; $p<0.001$). For the UVN+met group, we observed a significant decrease of the total distance travelled compared to the sham group at d1 (Tukey post-hoc; $p<0.01$), followed by a significant increase from d14 (Tukey post-hoc; $p<0.001$) to d30 (Tukey post-hoc; $p<0.001$).

3.2.4.2 Mean velocity during free locomotion

Regarding the mean velocity parameter, we observed a similar kinetics after UVN for both UVN+placebo and UVN+met groups (**Figure 8C**). Statistical analysis revealed significant 'time' and 'time x group'effects (two-way repeated measures ANOVA, 'time': $F(7,203)=121$, $p<0.001$; 'time x group': $F(14,203)=32.4$ $p<0.001$). A significant decrease was observed in the UVN+placebo group compared to the sham group from d1 (Tukey post-hoc; $p<0.001$) to d3 (Tukey post-hoc; $p<0.01$). The opposite was observed from d14 to d30 with a significant increase of the mean velocity (Tukey post-hoc; $p<0.001$) persisting at d30 (Tukey post-hoc; $p<0.001$). Similar results were

obtained in the UVN+met group with a significant decrease from d1 (Tukey post-hoc; $p<0.001$) to d3 (Tukey post-hoc; $p<0.01$) compared to the sham group. Again, the opposite was observed from d14 to d30 with a significant increase of the mean velocity (Tukey post-hoc; $p<0.001$) persisting at d30 (Tukey post-hoc; $p<0.001$).

3.2.4.3 Mean acceleration during free locomotion

Since vestibular receptors detect accelerations, this parameter is particularly relevant to assess vestibular dysfunction following UVN (Rastoldo et al., 2020). We observed a significant increase of this parameter after UVN for both UVN+placebo and UVN+met groups in the compensated phase (**Figure 8D**). Statistical analysis revealed significant 'time' and 'time x group' effects (two-way repeated measures ANOVA, 'time': $F(7,203)=39.4$, $p<0.001$; 'time x group': $F(14,203)=17.3$ $p<0.001$). A significant decrease was observed in the UVN+placebo group compared to the sham group at d1 (Tukey post-hoc; $p<0.05$) followed by a significant increase from d14 (Tukey post-hoc; $p<0.001$) to d30 (Tukey post-hoc; $p<0.001$). For the UVN+met group, we also observed a significant diminution compared with the sham group at d1 (Tukey post-hoc; $p<0.001$) persisting until d3 (Tukey post-hoc; $p<0.01$), followed by a significant increase at d14 (Tukey post-hoc; $p<0.001$) persisting until d30 (Tukey post-hoc; $p<0.001$).

4. Discussion

Due to their anti-inflammatory action, corticosteroids are the reference treatment for brain injuries and many inflammatory diseases, such as APV (Strupp et al., 2013; Strupp and Brandt, 2009b; Walker, 2009). We used methylprednisolone, a corticosteroid, to assess the functional role of the endogenous acute neuroinflammation process in a rodent model of UVN. Here, we demonstrate that acute

anti-inflammatory treatment has deleterious effects on vestibular compensation and disrupts the neuroplasticity mechanisms promoting functional recovery. Our results suggest for the first time a beneficial role of acute endogenous neuroinflammation in the expression of neuroplasticity mechanisms in the deafferented VN, promoting functional recovery after UVN.

4.1. Acute anti-inflammatory treatment alters adaptive post-lesional plasticity in the deafferented VNs after UVN.

Methylprednisolone is a synthetic corticosteroid, mimicking endogenous corticosteroids (EC) action on the GR, an ubiquitous receptor expressed in almost all cells in mammals. When activated by a ligand, GR undergoes translocation into the nucleus to regulate the expression of genes encoding a variety of inflammatory proteins exerting anti-inflammatory and immunosuppressive actions (Payne and Adcock, 2001; Rhen and Cidlowski, 2005). Interestingly, previous works reported the activation of the HPA axis after unilateral vestibular deafferentation (UVD) (Cameron and Dutia, 1999; Gliddon et al., 2003; Tighilet et al., 2009), leading to increased release of anti-inflammatory EC. Consistently, we observed an increased nuclear GR localization in the deafferented medial VNs after UVN. Although HPA axis activation after UVD is thought to be beneficial (for review see Saman et al., 2012), it has been reported that overexposure to corticosteroids has detrimental effects on vestibular compensation (Yamamoto, 2000). Following acute anti-inflammatory treatment, we observed a significant reduction of GR nuclear localization which is usually observed after desensitization of the receptor due to glucocorticoids overexposure (Numakawa et al., 2009). The association of the acute anti-inflammatory treatment with EC probably leads to high concentrations of glucocorticoids in the deafferented VNs.

669 The restoration of the electrophysical balance between ipsi- and contra-lesional VNs,
670 crucial for functional recovery, is supported at the cellular level by the expression of
671 many neuroplasticity mechanisms in the deafferented VNs. We assessed the impact
672 of acute anti-inflammatory treatment on post-lesional plasticity mechanisms by looking
673 first at the glial responses, considered as hallmarks of the inflammatory response in
674 the CNS. We observed that exposure to acute anti-inflammatory treatment significantly
675 reduces astroglial and microglial reactions in the deafferented VNs after UVN, as
676 previously shown for spinal cord injury (SCI) (Takeda et al., 2004). GR activation is
677 known to inhibit NF-kB, a key transcriptional factor for the inflammatory response (Liu
678 et al., 2017; Quax et al., 2013). The expression of NF-kB being crucial for microglial
679 and astroglial responses (Liddelow and Barres, 2017; Santa-Cecília et al., 2016), its
680 inhibition by EC's action on GR combined with acute anti-inflammatory treatment may
681 cause the massive decreased glial response in the deafferented VNs. Their inhibition
682 after acute anti-inflammatory treatment is associated with altered vestibular
683 compensation, probably highlighting their contribution to functional recovery. Glial
684 reactions are crucial for adaptative post-lesional plasticity mechanisms in the VNs,
685 since they promote preservation of tissue integrity and wound repair (Cherry et al.,
686 2014; Myer, 2006; Quintana, 2017) and modulate neuronal network excitability
687 through various mechanisms such as K^+ clearance (Bellot-Saez et al., 2017) and Brain-
688 Derived-Neurotrophic-Factor (BDNF) signaling (Coull et al., 2005; Ferrini and De
689 Koninck, 2013).
690
691 Neurogenesis is an adaptive mechanism promoting vestibular compensation (Dutheil
692 et al., 2009; Rastoldo et al., 2021). We observed that acute anti-inflammatory treatment
693 reduces cell proliferation and survival in deafferented medial VNs. Reduction of cell

proliferation was also reported after overexposure to glucocorticoids in the hippocampus (Anacker et al., 2013). Altered neurogenesis is known to be associated with impaired functional recovery after UVN (Dutheil et al., 2009) and probably contributes to the exacerbated and persistent functional deficits observed after acute anti-inflammatory treatment. This may involve GR's inhibition of NF-kB, which exerts a pro-proliferative effect on neural progenitors (Widera et al., 2006). An alternative explanation might concern the inhibition of glial reactions, usually promoting neurogenesis through the release of BDNF (Bath et al., 2012; Ekdahl et al., 2009).

Finally, we examined the impact of acute anti-inflammatory treatment on vestibular neurons' excitability in the deafferented VNs by focusing on GABAergic transmission. Our previous studies have shown that UVN induces a significant reduction of KCC2 expression in the deafferented lateral VNs (Dutheil et al., 2016), possibly leading to an intracellular accumulation of [Cl-] ions, inducing a depolarizing outward current through GABAA receptors (Coull et al., 2005, 2003). This mechanism likely plays a role in vestibular compensation through the transitory restoration of spontaneous activity in the deafferented VNs during the acute phase (Dutheil et al., 2016). Here we observed that acute anti-inflammatory treatment not only prevented KCC2 downregulation but significantly enhanced its expression in the deafferented lateral VNs. This phenomenon may induce an excitability deficit during the acute phase since KCC2 upregulation is likely associated with amplified inhibitory GABAergic transmission (Bos et al., 2013; Goulton et al., 2018; Lorenzo et al., 2020). KCC2 upregulation was also reported after SCI and administration of corticosteroids (Dai et al., 2018). The reactive microglia – BDNF - TrkB signaling was shown to be a main actor for KCC2 downregulation (Coull et al., 2005; Ferrini and De Koninck, 2013; Rivera, 2004; Rivera

et al., 2002). In accordance with this, we have previously shown that the administration of a TrkB receptor antagonist after UVN increases KCC2 expression (Dutheil et al., 2016). Interestingly, KCC2 upregulation is thought to involve a TrkB receptor mediator, the Phospholipase C gamma (PLCy) (Rivera, 2004; Tashiro et al., 2015). Previous works reported that glucocorticoids overexposure, as is likely the case after UVN and acute anti-inflammatory treatment, decreases PLCy binding to TrkB receptors (Numakawa et al., 2009) leading to KCC2 upregulation (Rivera, 2004; Tashiro et al., 2015). Interestingly, we observed that acute versus chronic treatment with muscimol, a GABAA receptor agonist, had antagonistic effects on vestibular compensation in UVN animals (Dutheil et al., 2013), highlighting the complex contribution of GABAergic signaling for functional recovery.

In conclusion, we demonstrate that reactive plasticity mechanisms generated in the deafferented vestibular nuclei after UVN strongly depend on the acute inflammatory state, since their expression is prevented after acute anti-inflammatory treatment. One could argue that these deleterious effects are not due to the anti-inflammatory role of the corticosteroids but rather to their action on the GR. Therefore, the use of nonsteroidal anti-inflammatory drugs (NSAIDs) may have different effects on post-lesional plasticity. This hypothesis was, however, refuted by a recent study (Golia et al., 2019), showing that high doses of ibuprofen, a NSAIDs, have deleterious consequences on hippocampal plasticity supporting the view that excessive inhibition of the inflammatory response impairs the expression of neural plasticity.

4.2 Acute anti-inflammatory treatment after UVN alters the expression of the vestibular syndrome as well as the kinetics of vestibular compensation.

To assess the consequences of acute anti-inflammatory treatment on functional recovery, we performed behavioral investigations to assess vestibular, postural and locomotor functions (Cassel et al., 2018; Marouane et al., 2020; Péricat et al., 2017; Rastoldo et al., 2020). It is now widely accepted that acute vestibular syndrome originates from electrophysiological asymmetry between intact and deafferented VN and that recovery occurs through rebalance of electrical activity (Tighilet and Chabbert, 2019). We used two behavioral tests that could assess the return to VNs electrophysiological homeostasis. First, we used a qualitative scale, listing typical postural and locomotor–deficits classically induced by UVN and known to reflect vestibular function impairment and recovery (Deliagina et al., 1997; Péricat et al., 2017). Then, we quantified the ipsilesional circling, a behavioral parameter observed in various rodent models of neuropathologies resulting from cerebral electrophysiological asymmetry (Löscher, 2010; Stiles and Smith, 2015). The acute administration of methylprednisolone exacerbates the severity of behavioral deficits in both tests. We can therefore assume that the acute anti-inflammatory treatment delays the return to electrophysiological homeostasis in the VNs and consequently, the vestibular compensation.

The VNs receive multimodal sensory inputs (vestibular, visual; tactile and proprioceptive) and play a crucial role in postural stability, balance control and reflex responses to body displacements through descending vestibulospinal pathways (see (McCall et al., 2017)for review). In the case of UVD, the loss of vestibular information

767 from ipsilesional VNs and the subsequent VNs electrophysiological asymmetry leads
768 to postural impairments (see Deliagina et al., 2006 for review) that we assessed
769 quantitatively. We observed, as previously described after UVN, an altered postural
770 function during the acute phase as attested by the increase in the mean body torsion,
771 the significant decrease of the rearing time and more unstable statokinesigrams
772 compared to the sham group 3 days after the lesion. With time, we observed a
773 progressive compensation of the postural parameters, concomitant with an increased
774 weight distribution towards the injured side. This phenomenon was described as a
775 compensatory mechanism, probably increasing tactile and proprioceptive inputs to the
776 deafferented VNs, leading to a sensory reweighting. Increased sensitivity of vestibular
777 neurons to proprioceptive inputs has been described after unilateral vestibular loss
778 (Jamali et al., 2014; Sadeghi et al., 2011) and is thought to support a sensory
779 substitution mechanism, which is known to play a role in the vestibular compensation
780 process (see Lacour et al., 2016 for review).
781 After acute methylprednisolone treatment, we observed enhanced short- and long-
782 term postural deficits probably involving different plasticity mechanisms. We observed
783 significantly enhanced body torsion toward the injured side during the acute phase but
784 also increased instability of the barycenter during the compensated phase. These
785 animals also exhibited significant and persistent use of the abdomen probably to
786 improve postural balance through a somaesthetic substitution process. This
787 hypothesis is supported by the measurement of the support surface after tail
788 suspension test (TST), showing a strong impairment in UVN+met animals even 1
789 month after UVN, whereas UVN+placebo animals recovered over time. Under TST
790 conditions, somaesthetic inputs are greatly reduced and the effectiveness of the
791 vestibulo-spinal reflex is principally under the control of the recovery of vestibular

792 function). We can argue that the long-term alteration of the plasticity mechanisms by
793 acute methylprednisolone treatment causes the long-term alteration of the
794 vestibulospinal reflex when mainly controlled by the vestibular function recovery.
795 Locomotor activity in rats after UVN was quantified in an automated and unbiased
796 manner under ecological conditions, through the use of different quantitative
797 parameters, recently validated as part of a specific posturo-locomotor phenotype after
798 UVN (Rastoldo et al., 2020). In accordance with previous works, we observed a
799 significant increase of these parameters with time, confirming the persistent
800 hyperactivity after vestibular loss (Lindner et al., 2019; Rastoldo et al., 2020). This
801 could represent a compensatory strategy since by increasing locomotion velocity,
802 automatic spinal networks inhibit misleading vestibular information (Fabre-Adinolfi et
803 al., 2018). As previously described in rat models of spinal cord injury (Haghighi et al.,
804 2000; Pereira et al., 2009; Yin et al., 2013), acute anti-inflammatory treatment with
805 methylprednisolone had no benefits for locomotion.
806
807 We argue that the acute treatment with methylprednisolone dysregulates the well-
808 controlled endogenous balance between pro- and anti-inflammatory signals after UVN,
809 leading to glucocorticoid overexposure. Acute methylprednisolone treatment alters
810 both short- and long-term plasticity expression in the deafferented VNs, inducing the
811 enhanced and persistent vestibular and postural deficits. Interestingly, the
812 inflammatory response was only blocked during the acute 3-day period after UVN but
813 had both long-term cellular and behavioral consequences. Taken together, these
814 results confirm the crucial role of this critical time period for functional recovery and
815 highlight its potential therapeutic role.
816

4.3 Clinical considerations

The UVN rodent model used in this work, displaying an acute phase of severe disorders, followed by a progressive reduction of the symptoms, faithfully mimics the vestibular syndrome encountered in most acute peripheral vestibulopathies (APV). Given its tissue correlation, it may be compared in first instance to vestibular neurotomy undertaken in the case of intractable Menière disease (Miyazaki et al., 2017; Nevoux et al., 2017), or vestibular schwannoma surgery (Halliday et al., 2018). In these two cases, central processes of vestibular neurons progressively degenerate through Wallerian degeneration, after being severed from their cell bodies located in the Scarpa's ganglion. Based on the observation of inflammatory markers in the vestibular nuclei of UVN rats, it can be assumed that similar inflammation may take place following neurotomy and vestibular schwannoma. Present results are therefore of interest for the pharmacological management of patients in these conditions. Administration of corticoids within the appropriate time windows, avoiding the acute phase, may optimize functional recovery and stimulate vestibular compensation processes.

Although systemic inflammation has been described in vestibular neuritis patients (Kassner et al., 2011), there is still no consistent evidence of a central inflammation in most cases (Hegemann and Wenzel, 2017; Uffer and Hegemann, 2016). Rather, an intralabyrinthine source is now favoured (Eliezer et al., 2019). It can be assumed that vestibular primary neurons that compose the vestibular nerve remain alive although disconnected from the vestibular sensory cells (Cassel et al., 2019; Tighilet et al., 2019). This situation differs slightly from the UVN model. However, among UVD models, chemical and surgical labyrinthectomy models have been reported to trigger inflammation and reactive plasticity mechanisms in the VNs (Campos Torres et al.,

1999; Campos-Torres et al., 2005; Dutheil et al., 2011; Liberge et al., 2010). The presence of a central inflammatory reaction in vestibular neuritis should therefore be considered and the administration of acute corticosteroids should be questioned.

One might then ask why some clinical studies have reported significant benefits of acute corticotherapy in APV (Ariyasu et al., 1990; Strupp et al., 2004). It should be noted that the reported effectiveness of corticotherapy has mainly been based on the measurement of the vestibulo-ocular-reflex gain on caloric tests and did not include scales measuring the quality of life nor posturography measurements, better able to quantify central vestibular compensation. Furthermore, those results are now contested since meta-analysis has questioned the long-term benefits of acute corticotherapy (Fishman et al., 2011; Goudakos et al., 2010; Solis et al., 2019), while recent studies proved no effectiveness of this treatment compared to vestibular re-education or other pharmacological treatment (Goudakos et al., 2014; Yoo et al., 2017).

The interest of understanding the inflammatory processes associated with vestibular pathologies extends well beyond the types of vestibular disorders mentioned above, as proinflammatory signatures have also been recently reported in Meniere disease and Vestibular Migraine (Flook et al., 2019). In conclusion, this study using the UVN model raises new questions regarding the early use of systemic corticosteroids for the treatment of APV in humans. Further clinical studies will be necessary to validate the benefits of a reduction of their systematic use in human, while preferring other pharmacological or re-educational therapies.

5. Conclusion

Our study proves, for the first time, that the pharmacological blockade of the acute inflammatory response after unilateral vestibular neurectomy alters the expression of the adaptative plasticity mechanisms in the ipsilesional VNs, involved in functional recovery. These results indicate that the endogenous acute neuroinflammation seems beneficial for vestibular compensation and question the use of corticosteroids in vestibular patients during the acute phase. The results also highlight a critical time window after the lesion since a treatment administrated during the acute phase has long-term effects.

6. List of abbreviations

Acute peripheral vestibulopathies (APV)

Central nervous system (CNS)

Unilateral vestibular deafferentation (UVD)

Unilateral vestibular neurectomy (UVN)

Vestibular nuclei (VNs)

Tumor necrosis factor-alpha (TNF-alpha)

Nuclear factor-kappa B (NF-kB)

Hypothalamo-pituitary-adrenal (HPA)

Endogenous corticosteroids (EC)

Intraperitoneally (i.p)

Days (d)

Methylprednisolone (met)

5-Bromo-2'-deoxyuridine (BrdU)

Phosphate buffer (PB)

Paraformaldehyde (PFA)

Glucocorticoid receptor (GR)

Ionized calcium-binding adapter molecule 1 (IBA1)

Potassium–chloride cotransporter 2 (KCC2)

Glial fibrillary acidic protein (GFAP)

Standard error mean (SEM)

Tail-Suspension Test (TST)

Equation (Equ)

Centimeters (cm)

Spinal cord injury (SCI)

Brain-Derived-Neurotrophic-Factor (BDNF)

Phospholipase C gamma (PLCy)

Non Steroidal Anti-Inflammatory Drugs (NSAIDs)

7. Declarations

Ethics approval and consent to participate

All experiments were performed in accordance with the National Institutes of Health's Guide for Care and Use of Laboratory Animals (NIH Publication no. 80-23) revised in 1996 for the UK Animals (Scientific Procedures) Act of 1986 and associated guidelines or the Policy on Ethics approved by the Society for Neuroscience in November 1989 and amended in November 1993 and under veterinary and National Ethical Committee supervision (French Agriculture Ministry Authorization: B13-055-25). The present study was specifically approved by Neurosciences Ethics Committee N°71 of the French National Committee of animal experimentation.

Consent for publication

Not applicable

Availability of data and materials

The datasets used and/or analysed during the current study are available from the corresponding author on reasonable request.

Competing interests

The authors declare that they have no competing interests.

Funding

This research was supported by grants from the Ministère de l'enseignement supérieur et de la recherche and CNRS (UMR 7260 Aix-Marseille Université).

Authors' contributions

B.T: Supervision; N.E. and B.T.: Conceptualization, Methodology, Investigation; N.E., I.W., G.R., E.M, A.T., D.P, F.S and B.T.: Formal Analysis; N.E, C.H., C.C, F.S and B.T.: Writing –Original Draft, Writing –Review & Editing.

Acknowledgements

We thank Elodie Mansour for taking care of the animals and Abdessadek El Ahmadi for expertise in statistical analysis.

8. References

Anacker, C., Cattaneo, A., Luoni, A., Musaelyan, K., Zunszain, P.A., Milanesi, E., Rybka, J., Berry, A., Cirulli, F., Thuret, S., Price, J., Riva, M.A., Gennarelli, M., Pariante, C.M., 2013. Glucocorticoid-Related Molecular Signaling Pathways Regulating Hippocampal Neurogenesis. Neuropsychopharmacol 38, 872–883. https://doi.org/10.1038/npp.2012.253

Ariyasu, L., Byl, F.M., Sprague, M.S., Adour, K.K., 1990. The Beneficial Effect of Methylprednisolone in Acute Vestibular Vertigo. Archives of Otolaryngology - Head and Neck Surgery 116, 700–703. https://doi.org/10.1001/archotol.1990.01870060058010

Bath, K.G., Akins, M.R., Lee, F.S., 2012. BDNF control of adult SVZ neurogenesis. Dev. Psychobiol. 54, 578–589. https://doi.org/10.1002/dev.20546

Bellot-Saez, A., Kékesi, O., Morley, J.W., Buskila, Y., 2017. Astrocytic modulation of neuronal excitability through K+ spatial buffering. Neuroscience & Biobehavioral Reviews 77, 87–97. https://doi.org/10.1016/j.neubiorev.2017.03.002

Beraneck, M., Hachemaoui, M., Idoux, E., Ris, L., Uno, A., Godaux, E., Vidal, P.-P., Moore, L.E., Vibert, N., 2003. Long-Term Plasticity of Ipsilesional Medial Vestibular Nucleus Neurons After Unilateral Labyrinthectomy. Journal of Neurophysiology 90, 184–203. https://doi.org/10.1152/jn.01140.2002

Bos, R., Sadlaoud, K., Boulenguez, P., Buttigieg, D., Liabeuf, S., Brocard, C., Haase, G., Bras, H., Vinay, L., 2013. Activation of 5-HT2A receptors upregulates the function of the neuronal K-Cl cotransporter KCC2. Proceedings of the National Academy of Sciences 110, 348–353. https://doi.org/10.1073/pnas.1213680110

Bracken, M.B., Collins, W.F., Freeman, D.F., Shepard, M.J., Wagner, F.W., Silten, R.M., Hellenbrand, K.G., Ransohoff, J., Hunt, W.E., Perot, P.L., Grossman, R.G., Green, B.A., Eisenberg, H.M., Rifkinson, N., Goodman, J.H., Meagher, J.N., Fischer, B., Clifton, G.L., Flamm, E.S., Rawe, S.E., 1984. Efficacy of Methylprednisolone in Acute Spinal Cord Injury. JAMA 251, 45–52. https://doi.org/10.1001/jama.1984.03340250025015

968 Bronstein, A.M., Dieterich, M., 2019. Long-term clinical outcome in vestibular neuritis: Current
969 Opinion in Neurology 32, 174–180. https://doi.org/10.1097/WCO.0000000000000652
970 Cameron, S.A., Dutia, M.B., 1999. Lesion-induced plasticity in rat vestibular nucleus neurones
971 dependent on glucocorticoid receptor activation. The Journal of Physiology 518, 151–
972 158. https://doi.org/10.1111/j.1469-7793.1999.0151r.x
973 Campos Torres, A., Vidal, P.P., de Waele, C., 1999. Evidence for a microglial reaction within
974 the vestibular and cochlear nuclei following inner ear lesion in the rat. Neuroscience
975 92, 1475–1490. https://doi.org/10.1016/S0306-4522(99)00078-0
976 Campos-Torres, A., Touret, M., Vidal, P.P., Barnum, S., de Waele, C., 2005. The differential
977 response of astrocytes within the vestibular and cochlear nuclei following unilateral
978 labyrinthectomy or vestibular afferent activity blockade by transtympanic tetrodotoxin
979 injection in the rat. Neuroscience 130, 853–865.
980 https://doi.org/10.1016/j.neuroscience.2004.08.052
981 Cassel, R., Bordiga, P., Carcaud, J., Simon, F., Beraneck, M., Gall, A.L., Benoit, A., Bouet, V.,
982 Philoxene, B., Besnard, S., Watabe, I., Pericat, D., Hautefort, C., Assie, A., Tonetto, A.,
983 Dyhrfjeld-Johnsen, J., Llorens, J., Tighilet, B., Chabbert, C., 2019. Morphological and
984 functional correlates of vestibular synaptic deafferentation and repair in a mouse model
985 of acute-onset vertigo. Disease Models & Mechanisms 12.
986 https://doi.org/10.1242/dmm.039115
987 Cassel, R., Bordiga, P., Pericat, D., Hautefort, C., Tighilet, B., Chabbert, C., 2018. New mouse
988 model for inducing and evaluating unilateral vestibular deafferentation syndrome.
989 Journal of Neuroscience Methods 293, 128–135.
990 https://doi.org/10.1016/j.jneumeth.2017.09.002
991 Cherry, J.D., Olschowka, J.A., O'Banion, M., 2014. Neuroinflammation and M2 microglia: the
992 good, the bad, and the inflamed. Journal of Neuroinflammation 11, 98.
993 https://doi.org/10.1186/1742-2094-11-98
994 Coull, J.A.M., Beggs, S., Boudreau, D., Boivin, D., Tsuda, M., Inoue, K., Gravel, C., Salter,
995 M.W., De Koninck, Y., 2005. BDNF from microglia causes the shift in neuronal anion

gradient underlying neuropathic pain. Nature 438, 1017–1021. https://doi.org/10.1038/nature04223

Coull, J.A.M., Boudreau, D., Bachand, K., Prescott, S.A., Nault, F., Sík, A., Koninck, P.D., Koninck, Y.D., 2003. Trans-synaptic shift in anion gradient in spinal lamina I neurons as a mechanism of neuropathic pain. Nature 424, 938–942. https://doi.org/10.1038/nature01868

Dai, S., Qi, Y., Fu, J., Li, N., Zhang, X., Zhang, J., Zhang, W., Xu, H., Zhou, H., Ma, Z., 2018. Dexmedetomidine attenuates persistent postsurgical pain by upregulating K⁺–Cl− cotransporter-2 in the spinal dorsal horn in rats. JPR Volume 11, 993–1004. https://doi.org/10.2147/JPR.S158737

Darlington, C.L., Smith, P.F., 2000. Molecular mechanisms of recovery from vestibular damage in mammals: recent advances. Progress in Neurobiology 62, 313–325. https://doi.org/10.1016/S0301-0082(00)00002-2

Deliagina, T.G., Orlovsky, G.N., Zelenin, P.V., Beloozerova, I.N., 2006. Neural Bases of Postural Control. Physiology 21, 216–225. https://doi.org/10.1152/physiol.00001.2006

Deliagina, T.G., Popova, L.B., Grant, G., 1997. The role of tonic vestibular input for postural control in rats. Arch Ital Biol 135, 239–261.

Dutheil, S., Brezun, J.M., Leonard, J., Lacour, M., Tighilet, B., 2009. Neurogenesis and astrogenesis contribution to recovery of vestibular functions in the adult cat following unilateral vestibular neurectomy: cellular and behavioral evidence. Neuroscience 164, 1444–1456. https://doi.org/10.1016/j.neuroscience.2009.09.048

Dutheil, S., Escoffier, G., Gharbi, A., Watabe, I., Tighilet, B., 2013. GABA $_A$ Receptor Agonist and Antagonist Alter Vestibular Compensation and Different Steps of Reactive Neurogenesis in Deafferented Vestibular Nuclei of Adult Cats. J. Neurosci. 33, 15555–15566. https://doi.org/10.1523/JNEUROSCI.5691-12.2013

Dutheil, S., Lacour, M., Tighilet, B., 2011. Neurogenic Potential of the Vestibular Nuclei and Behavioural Recovery Time Course in the Adult Cat Are Governed by the Nature of the

Vestibular Damage. PLoS ONE 6, e22262. https://doi.org/10.1371/journal.pone.0022262

Dutheil, S., Watabe, I., Sadlaoud, K., Tonetto, A., Tighilet, B., 2016. BDNF Signaling Promotes Vestibular Compensation by Increasing Neurogenesis and Remodeling the Expression of Potassium-Chloride Cotransporter KCC2 and GABA $_A$ Receptor in the Vestibular Nuclei. J. Neurosci. 36, 6199–6212. https://doi.org/10.1523/JNEUROSCI.0945-16.2016

Dutia, M.B., 2010. Mechanisms of vestibular compensation: recent advances: Current Opinion in Otolaryngology & Head and Neck Surgery 18, 420–424. https://doi.org/10.1097/MOO.0b013e32833de71f

Ekdahl, C.T., Kokaia, Z., Lindvall, O., 2009. Brain inflammation and adult neurogenesis: The dual role of microglia. Neuroscience, Brain - Immune Interactions in Acute and Chronic Brain Disorders 158, 1021–1029. https://doi.org/10.1016/j.neuroscience.2008.06.052

Eliezer, M., Maquet, C., Horion, J., Gillibert, A., Toupet, M., Bolognini, B., Magne, N., Kahn, L., Hautefort, C., Attyé, A., 2019. Detection of intralabyrinthine abnormalities using post-contrast delayed 3D-FLAIR MRI sequences in patients with acute vestibular syndrome. Eur Radiol 29, 2760–2769. https://doi.org/10.1007/s00330-018-5825-0

Fabre-Adinolfi, D., Parietti-Winkler, C., Pierret, J., Lassalle-Kinic, B., Frère, J., 2018. You are better off running than walking revisited: Does an acute vestibular imbalance affect muscle synergies? Human Movement Science 62, 150–160. https://doi.org/10.1016/j.humov.2018.10.010

Fehlings, M.G., Wilson, J.R., Cho, N., 2014. Methylprednisolone for the Treatment of Acute Spinal Cord Injury: Counterpoint. Neurosurgery 61, 36–42. https://doi.org/10.1227/NEU.0000000000000412

Ferrini, F., De Koninck, Y., 2013. Microglia Control Neuronal Network Excitability via BDNF Signalling. Neural Plasticity 2013, 1–11. https://doi.org/10.1155/2013/429815

1049 Fishman, J.M., Burgess, C., Waddell, A., 2011. Corticosteroids for the treatment of idiopathic
1050 acute vestibular dysfunction (vestibular neuritis). Cochrane Database of Systematic
1051 Reviews. https://doi.org/10.1002/14651858.CD008607.pub2
1052 Flook, M., Frejo, L., Gallego-Martinez, A., Martin-Sanz, E., Rossi-Izquierdo, M., Amor-Dorado,
1053 J.C., Soto-Varela, A., Santos-Perez, S., Batuecas-Caletrio, A., Espinosa-Sanchez,
1054 J.M., Pérez-Carpena, P., Martinez-Martinez, M., Aran, I., Lopez-Escamez, J.A., 2019.
1055 Differential Proinflammatory Signature in Vestibular Migraine and Meniere Disease.
1056 Front. Immunol. 10, 1229. https://doi.org/10.3389/fimmu.2019.01229
1057 Gliddon, C.M., Darlington, C.L., Smith, P.F., 2003. Activation of the hypothalamic–pituitary–
1058 adrenal axis following vestibular deafferentation in pigmented guinea pig. Brain
1059 Research 964, 306–310. https://doi.org/10.1016/S0006-8993(02)04086-6
1060 Golia, M.T., Poggini, S., Alboni, S., Garofalo, S., Ciano Albanese, N., Viglione, A., Ajmone-
1061 Cat, M.A., St-Pierre, A., Brunello, N., Limatola, C., Branchi, I., Maggi, L., 2019. Interplay
1062 between inflammation and neural plasticity: Both immune activation and suppression
1063 impair LTP and BDNF expression. Brain, Behavior, and Immunity
1064 S0889159118312388. https://doi.org/10.1016/j.bbi.2019.07.003
1065 Goudakos, J.K., Markou, K.D., Franco-Vidal, V., Vital, V., Tsaligopoulos, M., Darrouzet, V.,
1066 2010. Corticosteroids in the Treatment of Vestibular Neuritis: A Systematic Review and
1067 Meta-Analysis 31, 7.
1068 Goudakos, J.K., Markou, K.D., Psillas, G., Vital, V., Tsaligopoulos, M., 2014. Corticosteroids
1069 and Vestibular Exercises in Vestibular Neuritis: Single-blind Randomized Clinical Trial.
1070 JAMA Otolaryngol Head Neck Surg 140, 434. https://doi.org/10.1001/jamaoto.2014.48
1071 Goulton, C.S., Watanabe, M., Cheung, D.L., Wang, K.W., Oba, T., Khoshaba, A., Lai, D.,
1072 Inada, H., Eto, K., Nakamura, K., Power, J.M., Lewis, T.M., Housley, G.D., Wake, H.,
1073 Nabekura, J., Moorhouse, A.J., 2018. Conditional Upregulation of KCC2 selectively
1074 enhances neuronal inhibition during seizures. bioRxiv 253831.
1075 https://doi.org/10.1101/253831

Haghighi, S.S., Agrawal, S.K., Surdell, D., Plambeck, R., Agrawal, S., Johnson, G.C., Walker, A., 2000. Effects of methylprednisolone and MK-801 on functional recovery after experimental chronic spinal cord injury. Spinal Cord 38, 733–740. https://doi.org/10.1038/sj.sc.3101074

Halliday, J., Rutherford, S.A., McCabe, M.G., Evans, D.G., 2018. An update on the diagnosis and treatment of vestibular schwannoma. Expert Rev Neurother 18, 29–39. https://doi.org/10.1080/14737175.2018.1399795

Hegemann, S.C.A., Wenzel, A., 2017. Diagnosis and Treatment of Vestibular Neuritis/Neuronitis or Peripheral Vestibulopathy (PVP)? Open Questions and Possible Answers: Otology & Neurotology 38, 626–631. https://doi.org/10.1097/MAO.0000000000001396

Hurlbert, R.J., 2000. Methylprednisolone for acute spinal cord injury: an inappropriate standard of care. Journal of Neurosurgery: Spine 93, 1–7. https://doi.org/10.3171/spi.2000.93.1.0001

Jamali, M., Mitchell, D.E., Dale, A., Carriot, J., Sadeghi, S.G., Cullen, K.E., 2014. Neuronal detection thresholds during vestibular compensation: contributions of response variability and sensory substitution: Neuronal detection thresholds during vestibular compensation. The Journal of Physiology 592, 1565–1580. https://doi.org/10.1113/jphysiol.2013.267534

Kassner, S.S., Schöttler, S., Bonaterra, G.A., Stern-Straeter, J., Hormann, K., Kinscherf, R., Gössler, U.R., 2011. Proinflammatory Activation of Peripheral Blood Mononuclear Cells in Patients with Vestibular Neuritis. Audiology and Neurotology 16, 242–247. https://doi.org/10.1159/000320839

Lacour, M., Helmchen, C., Vidal, P.-P., 2016. Vestibular compensation: the neuro-otologist's best friend. J Neurol 263, 54–64. https://doi.org/10.1007/s00415-015-7903-4

Lacour, M., Tighilet, B., 2010. Plastic events in the vestibular nuclei during vestibular compensation: The brain orchestration of a "deafferentation" code.

Restorative Neurology and Neuroscience 28, 19–35. https://doi.org/10.3233/RNN-2010-0509

Lacour, M., Xerri, C., 1980. Compensation of postural reactions to free-fall in the vestibular neurectomized monkey. Exp Brain Res 40, 103–110. https://doi.org/10.1007/BF00236668

Li, H., Godfrey, D.A., Rubin, A.M., 1995. Comparison of surgeries for removal of primary vestibular inputs: A combined anatomical and behavioral study in rats. The Laryngoscope 105, 417–424. https://doi.org/10.1288/00005537-199504000-00015

Liberge, M., Manrique, C., Bernard-Demanze, L., Lacour, M., 2010. Changes in TNFa, NF B and MnSOD protein in the vestibular nuclei after unilateral vestibular deafferentation 16.

Liddelow, S.A., Barres, B.A., 2017. Reactive Astrocytes: Production, Function, and Therapeutic Potential. Immunity 46, 957–967. https://doi.org/10.1016/j.immuni.2017.06.006

Lindner, M., Gosewisch, A., Eilles, E., Branner, C., Krämer, A., Oos, R., Wolf, E., Ziegler, S., Bartenstein, P., Brandt, T., Dieterich, M., Zwergal, A., 2019. Ginkgo biloba Extract EGb 761 Improves Vestibular Compensation and Modulates Cerebral Vestibular Networks in the Rat. Front. Neurol. 10, 147. https://doi.org/10.3389/fneur.2019.00147

Liu, T., Zhang, L., Joo, D., Sun, S.-C., 2017. NF-κB signaling in inflammation. Sig Transduct Target Ther 2, 17023. https://doi.org/10.1038/sigtrans.2017.23

Lorenzo, L.-E., Godin, A.G., Ferrini, F., Bachand, K., Plasencia-Fernandez, I., Labrecque, S., Girard, A.A., Boudreau, D., Kianicka, I., Gagnon, M., Doyon, N., Ribeiro-da-Silva, A., De Koninck, Y., 2020. Enhancing neuronal chloride extrusion rescues α2/α3 GABA A -mediated analgesia in neuropathic pain. Nature Communications 11, 869. https://doi.org/10.1038/s41467-019-14154-6

Löscher, W., 2010. Abnormal circling behavior in rat mutants and its relevance to model specific brain dysfunctions. Neuroscience & Biobehavioral Reviews 34, 31–49. https://doi.org/10.1016/j.neubiorev.2009.07.001

Marouane, E., Rastoldo, G., El Mahmoudi, N., Péricat, D., Chabbert, C., Artzner, V., Tighilet, B., 2020. Identification of New Biomarkers of Posturo-Locomotor Instability in a Rodent Model of Vestibular Pathology. Front Neurol 11. https://doi.org/10.3389/fneur.2020.00470

Mccabe, B.F., Ryu, J.H., 1969. Experiments on vestibular compensation. The Laryngoscope 79, 1728–1736. https://doi.org/10.1288/00005537-196910000-00004

McCall, A.A., Miller, D.M., Yates, B.J., 2017. Descending Influences on Vestibulospinal and Vestibulosympathetic Reflexes. Front. Neurol. 8. https://doi.org/10.3389/fneur.2017.00112

Miyazaki, H., Nomura, Y., Mardassi, A., Deveze, A., Miura, M., Jike, M., Magnan, J., 2017. How minimally invasive vestibular neurotomy for incapacitating Meniere's disease improves dizziness and anxiety. Acta Otolaryngol 137, 707–711. https://doi.org/10.1080/00016489.2017.1278790

Myer, D.J., 2006. Essential protective roles of reactive astrocytes in traumatic brain injury. Brain 129, 2761–2772. https://doi.org/10.1093/brain/awl165

Nevoux, J., Franco-Vidal, V., Bouccara, D., Parietti-Winkler, C., Uziel, A., Chays, A., Dubernard, X., Couloigner, V., Darrouzet, V., Mom, T., Groupe de Travail de la SFORL, 2017. Diagnostic and therapeutic strategy in Menière's disease. Guidelines of the French Otorhinolaryngology-Head and Neck Surgery Society (SFORL). Eur Ann Otorhinolaryngol Head Neck Dis 134, 441–444. https://doi.org/10.1016/j.anorl.2016.12.003

Numakawa, T., Kumamaru, E., Adachi, N., Yagasaki, Y., Izumi, A., Kunugi, H., 2009. Glucocorticoid receptor interaction with TrkB promotes BDNF-triggered PLC- signaling for glutamate release via a glutamate transporter. Proceedings of the National Academy of Sciences 106, 647–652. https://doi.org/10.1073/pnas.0800888106

Paragliola, R.M., Papi, G., Pontecorvi, A., Corsello, S.M., 2017. Treatment with Synthetic Glucocorticoids and the Hypothalamus-Pituitary-Adrenal Axis. IJMS 18, 2201. https://doi.org/10.3390/ijms18102201

Paxinos, G., Watson, C., 2009. The rat brain in stereotaxic coordinates. Elsevier, Amsterdam; Boston.

Payne, D.N.R., Adcock, I.M., 2001. Molecular mechanisms of corticosteroid actions. Paediatric Respiratory Reviews 2, 145–150. https://doi.org/10.1053/prrv.2000.0122

Pereira, J.E., Costa, L.M., Cabrita, A.M., Couto, P.A., Filipe, V.M., Magalhães, L.G., Fornaro, M., Di Scipio, F., Geuna, S., Maurício, A.C., Varejão, A.S.P., 2009. Methylprednisolone fails to improve functional and histological outcome following spinal cord injury in rats. Experimental Neurology 220, 71–81. https://doi.org/10.1016/j.expneurol.2009.07.030

Péricat, D., Farina, A., Agavnian-Couquiaud, E., Chabbert, C., Tighilet, B., 2017. Complete and irreversible unilateral vestibular loss: A novel rat model of vestibular pathology. Journal of Neuroscience Methods 283, 83–91. https://doi.org/10.1016/j.jneumeth.2017.04.001

Precht, W., Shimazu, H., Markham, C.H., 1966. A mechanism of central compensation of vestibular function following hemilabyrinthectomy. Journal of Neurophysiology 29, 996–1010. https://doi.org/10.1152/jn.1966.29.6.996

Quax, R.A., Manenschijn, L., Koper, J.W., Hazes, J.M., Lamberts, S.W.J., van Rossum, E.F.C., Feelders, R.A., 2013. Glucocorticoid sensitivity in health and disease. Nature Reviews Endocrinology 9, 670–686. https://doi.org/10.1038/nrendo.2013.183

Quintana, F.J., 2017. Astrocytes to the rescue! Glia limitans astrocytic endfeet control CNS inflammation. Journal of Clinical Investigation 127, 2897–2899. https://doi.org/10.1172/JCI95769

Rastoldo, G., 2021. Adult and endemic neurogenesis in the vestibular nuclei after unilateral vestibular neurectomy. Progress in Neurobiology 11.

Rastoldo, G., El Mahmoudi, N., Marouane, E., Pericat, D., Watabe, I., Toneto, A., López-Juárez, A., Chabbert, C., Tighilet, B., 2021. Adult and endemic neurogenesis in the vestibular nuclei after unilateral vestibular neurectomy. Progress in Neurobiology 196, 101899. https://doi.org/10.1016/j.pneurobio.2020.101899

Rastoldo, G., Marouane, E., El Mahmoudi, N., Péricat, D., Bourdet, A., Timon-David, E., Dumas, O., Chabbert, C., Tighilet, B., 2020. Quantitative Evaluation of a New Posturo-Locomotor Phenotype in a Rodent Model of Acute Unilateral Vestibulopathy. Front. Neurol. 11. https://doi.org/10.3389/fneur.2020.00505

Rhen, T., Cidlowski, J.A., 2005. Antiinflammatory Action of Glucocorticoids — New Mechanisms for Old Drugs. N Engl J Med 353, 1711–1723. https://doi.org/10.1056/NEJMra050541

Rivera, C., 2004. Mechanism of Activity-Dependent Downregulation of the Neuron-Specific K-Cl Cotransporter KCC2. Journal of Neuroscience 24, 4683–4691. https://doi.org/10.1523/JNEUROSCI.5265-03.2004

Rivera, C., Li, H., Thomas-Crusells, J., Lahtinen, H., Viitanen, T., Nanobashvili, A., Kokaia, Z., Airaksinen, M.S., Voipio, J., Kaila, K., Saarma, M., 2002. BDNF-induced TrkB activation down-regulates the K+–Cl− cotransporter KCC2 and impairs neuronal Cl− extrusion. Journal of Cell Biology 159, 747–752. https://doi.org/10.1083/jcb.200209011

Russo, M.V., McGavern, D.B., 2016. Inflammatory neuroprotection following traumatic brain injury. Science 353, 783–785. https://doi.org/10.1126/science.aaf6260

Sadeghi, S.G., Minor, L.B., Cullen, K.E., 2011. Multimodal Integration After Unilateral Labyrinthine Lesion: Single Vestibular Nuclei Neuron Responses and Implications for Postural Compensation. Journal of Neurophysiology 105, 661–673. https://doi.org/10.1152/jn.00788.2010

Saman, Y., Bamiou, D.E., Gleeson, M., Dutia, M.B., 2012. Interactions between Stress and Vestibular Compensation – A Review. Front. Neur. 3. https://doi.org/10.3389/fneur.2012.00116

Santa-Cecília, F.V., Socias, B., Ouidja, M.O., Sepulveda-Diaz, J.E., Acuña, L., Silva, R.L., Michel, P.P., Del-Bel, E., Cunha, T.M., Raisman-Vozari, R., 2016. Doxycycline Suppresses Microglial Activation by Inhibiting the p38 MAPK and NF-kB Signaling Pathways. Neurotox Res 29, 447–459. https://doi.org/10.1007/s12640-015-9592-2

Shupak, A., Issa, A., Golz, A., Margalit Kaminer, Braverman, I., 2008. Prednisone Treatment for Vestibular Neuritis. Otology & Neurotology 29, 368–374. https://doi.org/10.1097/MAO.0b013e3181692804

Simon, F., Pericat, D., Djian, C., Fricker, D., Denoyelle, F., Beraneck, M., 2020. Surgical techniques and functional evaluation for vestibular lesions in the mouse: unilateral labyrinthectomy (UL) and unilateral vestibular neurectomy (UVN). J Neurol. https://doi.org/10.1007/s00415-020-09960-8

Smith, P.F., Curthoys, I.S., 1989. Mechanisms of recovery following unilateral labyrinthectomy: a review. Brain Research Reviews 14, 155–180. https://doi.org/10.1016/0165-0173(89)90013-1

Sochocka, M., Diniz, B.S., Leszek, J., 2017. Inflammatory Response in the CNS: Friend or Foe? Molecular Neurobiology 54, 8071–8089. https://doi.org/10.1007/s12035-016-0297-1

Solis, R.N., Sun, D.Q., Tatro, E., Hansen, M.R., 2019. Do steroids improve recovery in vestibular neuritis?: Steroids for Vestibular Neuritis. The Laryngoscope 129, 288–290. https://doi.org/10.1002/lary.27278

Stiles, L., Smith, P.F., 2015. The vestibular–basal ganglia connection: Balancing motor control. Brain Research 1597, 180–188. https://doi.org/10.1016/j.brainres.2014.11.063

Streit, W.J., Mrak, R.E., Griffin, W.S.T., 2004. [No title found]. J Neuroinflammation 1, 14. https://doi.org/10.1186/1742-2094-1-14

Strupp, M., Brandt, T., 2009a. Vestibular Neuritis. Semin Neurol 29, 509–519. https://doi.org/10.1055/s-0029-1241040

Strupp, M., Brandt, T., 2009b. Review: Current treatment of vestibular, ocular motor disorders and nystagmus. Ther Adv Neurol Disord 2, 223–239. https://doi.org/10.1177/1756285609103120

Strupp, M., Dieterich, M., Brandt, T., 2013. The Treatment and Natural Course of Peripheral and Central Vertigo. Deutsches Aerzteblatt Online. https://doi.org/10.3238/arztebl.2013.0505

1241 Strupp, M., Mandalà, M., López-Escámez, J.A., 2019. Peripheral vestibular disorders: an
1242 update. Current Opinion in Neurology 32, 165–173.
1243 https://doi.org/10.1097/WCO.0000000000000649
1244 Strupp, M., Zingler, V.C., Arbusow, V., Niklas, D., Maag, K.P., Dieterich, M., Bense, S., Theil,
1245 D., Jahn, K., Brandt, T., 2004. Methylprednisolone, Valacyclovir, or the Combination
1246 for Vestibular Neuritis. N Engl J Med 351, 354–361.
1247 https://doi.org/10.1056/NEJMoa033280
1248 Takeda, K., Sawamura, S., Sekiyama, H., Tamai, H., Hanaoka, K., 2004. Effect of
1249 Methylprednisolone on Neuropathic Pain and Spinal Glial Activation in Rats:
1250 Anesthesiology 100, 1249–1257. https://doi.org/10.1097/00000542-200405000-00029
1251 Tashiro, S., Shinozaki, M., Mukaino, M., Renault-Mihara, F., Toyama, Y., Liu, M., Nakamura,
1252 M., Okano, H., 2015. BDNF Induced by Treadmill Training Contributes to the
1253 Suppression of Spasticity and Allodynia After Spinal Cord Injury via Upregulation of
1254 KCC2. Neurorehabil Neural Repair 29, 677–689.
1255 https://doi.org/10.1177/1545968314562110
1256 Tighilet, B., Bordiga, P., Cassel, R., Chabbert, C., 2019. Peripheral vestibular plasticity vs
1257 central compensation: evidence and questions. J Neurol 266, 27–32.
1258 https://doi.org/10.1007/s00415-019-09388-9
1259 Tighilet, B., Brezun, J.M., Dit Duflo Sylvie, G., Gaubert, C., Lacour, M., 2007. New neurons in
1260 the vestibular nuclei complex after unilateral vestibular neurectomy in the adult cat:
1261 Reactive neurogenesis in adult vestibular lesioned cats. European Journal of
1262 Neuroscience 25, 47–58. https://doi.org/10.1111/j.1460-9568.2006.05267.x
1263 Tighilet, B., Chabbert, C., 2019. Adult neurogenesis promotes balance recovery after
1264 vestibular loss. Progress in Neurobiology 174, 28–35.
1265 https://doi.org/10.1016/j.pneurobio.2019.01.001
1266 Tighilet, B., Dutheil, S., Siponen, M.I., Noreña, A.J., 2016. Reactive Neurogenesis and Down-
1267 Regulation of the Potassium-Chloride Cotransporter KCC2 in the Cochlear Nuclei after

Cochlear Deafferentation. Front. Pharmacol. 7. https://doi.org/10.3389/fphar.2016.00281

Tighilet, B., Leonard, J., Bernard-Demanze, L., Lacour, M., 2015. Comparative analysis of pharmacological treatments with N-acetyl-dl-leucine (Tanganil) and its two isomers (N-acetyl-L-leucine and N-acetyl-D-leucine) on vestibular compensation: Behavioral investigation in the cat. European Journal of Pharmacology 769, 342–349. https://doi.org/10.1016/j.ejphar.2015.11.041

Tighilet, B., Manrique, C., Lacour, M., 2009. Stress axis plasticity during vestibular compensation in the adult cat. Neuroscience 160, 716–730. https://doi.org/10.1016/j.neuroscience.2009.02.070

Tighilet, B., Péricat, D., Frelat, A., Cazals, Y., Rastoldo, G., Boyer, F., Dumas, O., Chabbert, C., 2017. Adjustment of the dynamic weight distribution as a sensitive parameter for diagnosis of postural alteration in a rodent model of vestibular deficit. PLoS ONE 12, e0187472. https://doi.org/10.1371/journal.pone.0187472

Uffer, D.S., Hegemann, S.C.A., 2016. About the pathophysiology of acute unilateral vestibular deficit – vestibular neuritis (VN) or peripheral vestibulopathy (PVP)? VES 26, 311–317. https://doi.org/10.3233/VES-160581

Vidal, P.P., Wang, D.H., Graf, W., de Waele, C., 1993. Chapter 22 Vestibular control of skeletal geometry in the guinea pig: a problem of good trim?, in: Progress in Brain Research. Elsevier, pp. 229–243. https://doi.org/10.1016/S0079-6123(08)62282-7

Walker, M.F., 2009. Treatment of vestibular neuritis. Curr Treat Options Neurol 11, 41–45. https://doi.org/10.1007/s11940-009-0006-8

Widera, D., Mikenberg, I., Elvers, M., Kaltschmidt, C., Kaltschmidt, B., 2006. Tumor necrosis factor α triggers proliferation of adult neural stem cells via IKK/NF-κB signaling. BMC Neuroscience 7, 64. https://doi.org/10.1186/1471-2202-7-64

Yamamoto, T., 2000. The Effect of Stress Application on Vestibular Compensation. Acta Oto-Laryngologica 120, 504–507. https://doi.org/10.1080/000164800750046009

Yin, Y., Sun, W., Li, Z., Zhang, B., Cui, H., Deng, L., Xie, P., Xiang, J., Zou, J., 2013. Effects of combining methylprednisolone with rolipram on functional recovery in adult rats following spinal cord injury. Neurochemistry International 62, 903–912. https://doi.org/10.1016/j.neuint.2013.03.005

Yoo, M.H., Yang, C.J., Kim, S.A., Park, M.J., Ahn, J.H., Chung, J.W., Park, H.J., 2017. Efficacy of steroid therapy based on symptomatic and functional improvement in patients with vestibular neuritis: a prospective randomized controlled trial. Eur Arch Otorhinolaryngol 274, 2443–2451. https://doi.org/10.1007/s00405-017-4556-1

9. Figures legends

Figure1: The vestibular compensation: a model a post-lesional neuroplasticity and functional recovery.

Unilateral vestibular deafferentation (UDV) leads to a vestibular syndrome the origin of which is thought to be an electrophysiological imbalance between the ipsi- and contra-lesional vestibular nuclei (VNs). UVD leads to the emergence of a plethora of plasticity mechanisms in the ipsilesional VNs, supporting the progressive restoration of the electrophysiological balance and the subsequent functional recovery, called vestibular compensation.

Figure 2: Study design

Experimental protocol to study and visualize the impact of the pharmacological blockage of the acute neuroinflammation after UVN on the expression of the plasticity mechanisms observed in the deafferented VN, as well as on the kinetics on functional recovery in the adult rat.

S.: sacrifice

i.p: intraperitoneal injections

TST: Tail Suspension Test

Figure 3: Glial reactions in the medial vestibular nuclei (VNs) are blocked by the acute anti-inflammatory treatment after UVN.

A. Confocal analysis of microglial cells immunostained with IBA1 and DAPI (nucleus) in the deafferented medial VNs of a representative animal in sham, UVN+placebo and UVN+methylprednisolone (UVN+met) groups at d3 and d30 post UVN. Scale bar, 50mm. N=4 animals per group. **B.** Histograms showing the effects of vestibular lesion combined with placebo or acute anti-inflammatory treatment on the number of IBA1 immunoreactive cells in the deafferented medial VNs at d3 and d30 post UVN. **C**. Confocal analysis of astroglial cells immunostained with GFAP and DAPI (nucleus) in the deafferented medial VNs of a representative animal in sham, UVN+placebo and UVN+met groups at d3 and d30 post UVN. Scale bar, 50mm. N=4 animals per group. **D.** Histograms showing the effects of vestibular lesion combined with placebo or acute anti-inflammatory treatment on the number of GFAP immunoreactive cells in the deafferented MVN at d3 and d30 post UVN.

Each data point represents the mean number of immunoreactive cells, with error bars representing SEM. *p < 0,05; ** p < 0,01; ***p<0,001, 2 two-way ANOVA, post-hoc Tukey: *sham and UVN+placebo comparison. *sham and UVN+met comparison. *UVN+placebo and UVN+met comparison.

Figure 4: Glucocorticoid receptor (GR) localization, KCC2 expression, cell proliferation and survival are altered by the acute anti-inflammatory treatment after UVN.

A. Confocal analysis of GR and nucleus (DAPI) localization in the deafferented medial VNs of a representative animal in sham, UVN+placebo and UVN+met groups at d3 and d30 post UVN. Scale bar, 50mm. N=4 animals per group. **D.** Histograms showing the effects of vestibular lesion combined with placebo or acute anti-inflammatory treatment on the mean percentage of GR nuclear localization, quantified by the percentage of GR/DAPI ir-cells in the deafferented medial VNs at d3 and d30 post UVN. **C**. Confocal analysis of KCC2 expression in the deafferented medial VNs of a representative animal in sham, UVN+placebo and UVN+met groups at d3 and d30 post UVN. Scale bar, 20mm. N=4 animals per group. **D.** Histograms showing the effects of the lesion combined with placebo or acute anti-inflammatory treatment on the mean KCC2 immunofluorescence intensity in the deafferented medial VNs at d3 and d30 post UVN. **E**. Confocal analysis of proliferative cells immunostained with BrdU in the deafferented medial VNs of a representative animal in sham, UVN+placebo and UVN+met groups at d3 and d30 post UVN. Scale bar, 50mm. N=4 animals per group. **F.** Histograms showing the effects of the lesion combined with placebo or acute anti-inflammatory treatment on the number of Brdu immunoreactive cells in the deafferented medial VNs at d3 and d30 post UVN.

Each data point represents the mean number of immunoreactive cells, with error bars representing SEM. *p < 0,05; ** p < 0,01; ***p<0,001, 2 two-way ANOVA, post-hoc Tukey: *sham and UVN+placebo comparison. *sham and UVN+met comparison. *UVN+placebo and UVN+met comparison

Figure 5: Acute anti-inflammatory after UVN treatment exacerbates vestibular syndrome intensity and postural instability during vestibulo-spinal reflex after UVN

A. Illustration of the assessment grid used to conduct the qualitative analysis. **B**. Results representing the progression of the qualitative score along post-operative time for each group. **C**. Pictures of the support surface of a representative animal at d3 for each group. For each rat, a measurement was taken during the preoperative time to serve as baseline so that each rat acts as its own control. Data were normalized according to the baseline for every time-point. **D**. Results representing the changes of the support surface measured after tail suspension test (TST), reflecting the effectiveness of the vestibulospinal reflex along post-operative time for each group.
A red box is applied on the curve to illustrate the acute time window of the vestibular syndrome (d1 to d3) where the treatments were administrated daily. Each data point represents the mean for each group with error bars representing SEM. *p < 0,05; ** p < 0,01; ***p<0,001, 2 two-way ANOVA, post-hoc Tukey: *sham and UVN+placebo comparison. *sham and UVN+met comparison. *UVN+placebo and UVN+met comparison.

Figure 6: Acute anti-inflammatory treatment effects on weight distribution after UVN

A. Results representing the changes of the lateral weight distribution index along post-operative time for each group. Positive values indicate an increase of the weight on the right paws, negative values indicate an increase of the weight on the left paws. **B**.

Results representing the evolution of the rearing time (i.e, time spent on two paws) along post-operative time for each group.

A red box is applied on the curve to illustrate the acute time window of the vestibular syndrome (d1 to d3) where the treatments were administrated daily.

C. Results representing the ipsilesional circling behavior (i.e left circling).

Each data point represents the mean for each group with error bars representing SEM. *p < 0,05; ** p < 0,01; ***p<0,001, 2 two-way ANOVA, post-hoc Tukey: *sham and UVN+placebo comparison. *sham and UVN+met comparison. *UVN+placebo and UVN+met comparison

Figure 7: Acute anti-inflammatory treatment alters long-term postural recovery after UVN

A. Statokinesigrams illustrating the kinetics of barycenter and paw positions at d3 and d30 for a representative animal in the sham, UVN+placebo and UVN+met groups. For each statokinesigram, the antero-posterior axis is on the abscissa and the lateral axis on the ordinate. The dark blue, red, light blue and pink dot clouds are the traces of the average positions, respectively, of the right rear paws, left rear paws, right front and left front paws during a session at each moment when the animal is static on its four legs. The green point cloud is the trace of the successive positions of the barycentre calculated at each of these moments. The various black crosses represent the average position of the legs during an entire session. The red dot represents the average position of the barycentre during a session. **B**. Results representing the changes of the weight distributed on the abdomen, in grams, normalized by subtracting the preoperative value for each rat. **C**. Results representing changes of the mean lateral position of the barycenter, in centimeters, normalized by subtracting the preoperative value for each rat. **D.** Results representing changes of the barycenter inertia, an

indicator of the barycenter stability. For each rat, measurements were normalized as a ratio of the preoperative value. **E.** Results representing changes in the barycenter's lateral maximum deviation, an indicator of barycenter stability along the lateral axis. For each rat, measurements were normalized as a ratio of the preoperative value.

Each data point represents the mean for each group with error bars representing SEM. *p < 0,05; ** p < 0,01; ***p<0,001, 2 two-way ANOVA, post-hoc Tukey: *sham and UVN+placebo comparison. *sham and UVN+met comparison. *UVN+placebo and UVN+met comparison.

Figure 8: Acute anti-inflammatory treatment exacerbates postural alteration and has no beneficial effects on locomotion after UVN

A. Results representing changes in the mean body torsion, in degrees, along post-operative time for each group, normalized by subtracting the pre-operative value for each rat. Positives values indicate an increase in body torsion toward the left side while negative values indicate an increase towards the right side. **B.** Results representing changes in the total distance moved along post-operative time for each group, normalized as a ratio of the pre-operative value. **C**. Results representing changes in the mean velocity along post-operative time for each group, normalized as a ratio of the pre-operative value. **D**. Results representing changes in the mean acceleration along post-operative time for each group, normalized as a ratio of the pre-operative value.

A red box is applied on the curve to illustrate the acute time window of the vestibular syndrome (d1 to d3) where the treatments were administrated daily. Each data point represents the mean for each group with error bars representing SEM. *p < 0,05; ** p < 0,01; ***p<0,001, 2 two-way ANOVA, post-hoc Tukey: *sham and UVN+placebo

comparison. *sham and UVN+met comparison. *UVN+placebo and UVN+met comparison.

Figures

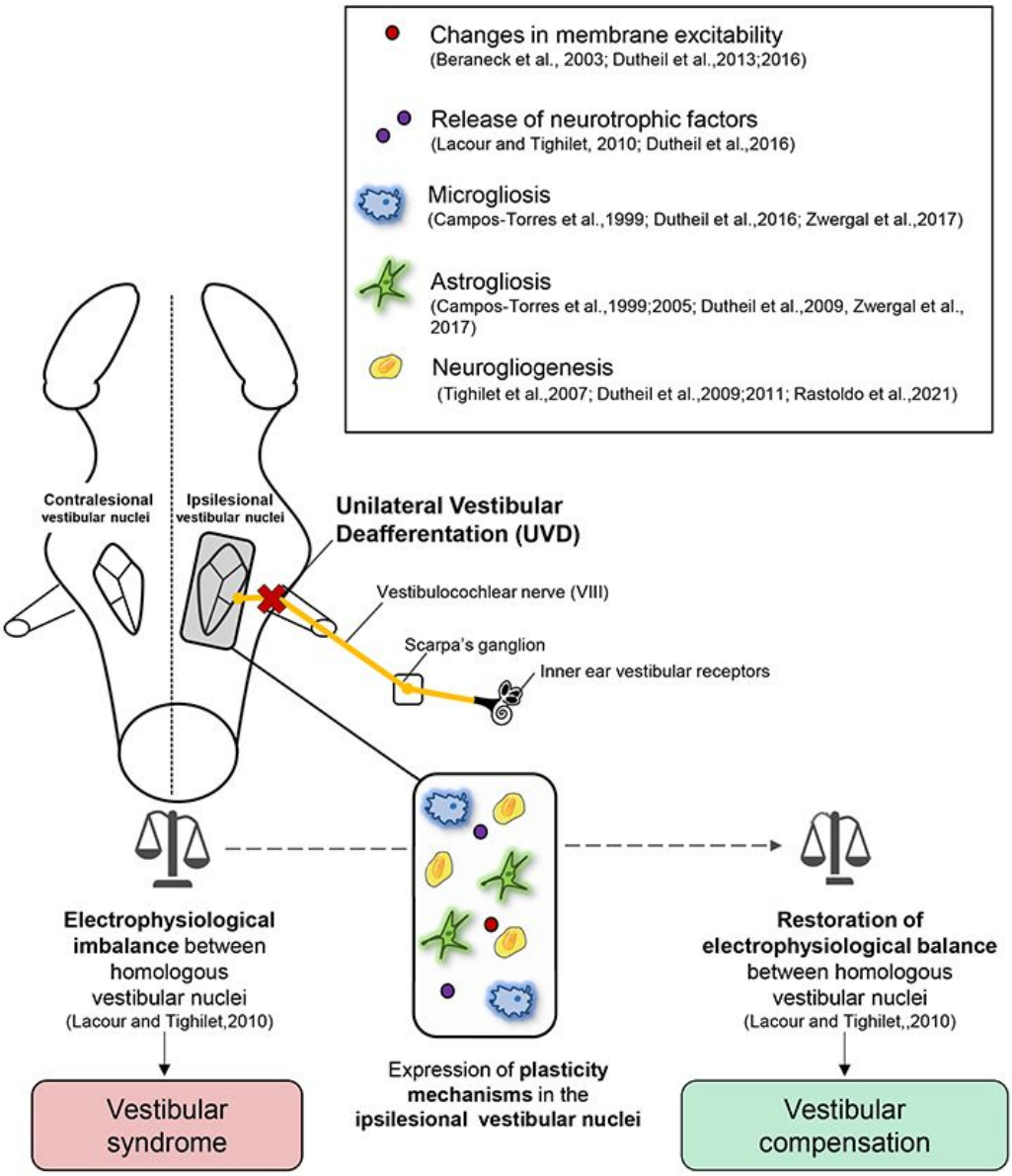

Figure 1

The vestibular compensation: a model a post-lesional 1305 neuroplasticity and functional recovery. Unilateral vestibular deafferentation (UDV) leads to a vestibular syndrome the origin of which is thought to be an electrophysiological imbalance between the ipsi- and contra-lesional vestibular nuclei (VNs).

UVD leads to the emergence of a plethora of plasticity mechanisms in the ipsilesional VNs, supporting the progressive restoration of the electrophysiological balance and the subsequent functional recovery, called vestibular compensation.

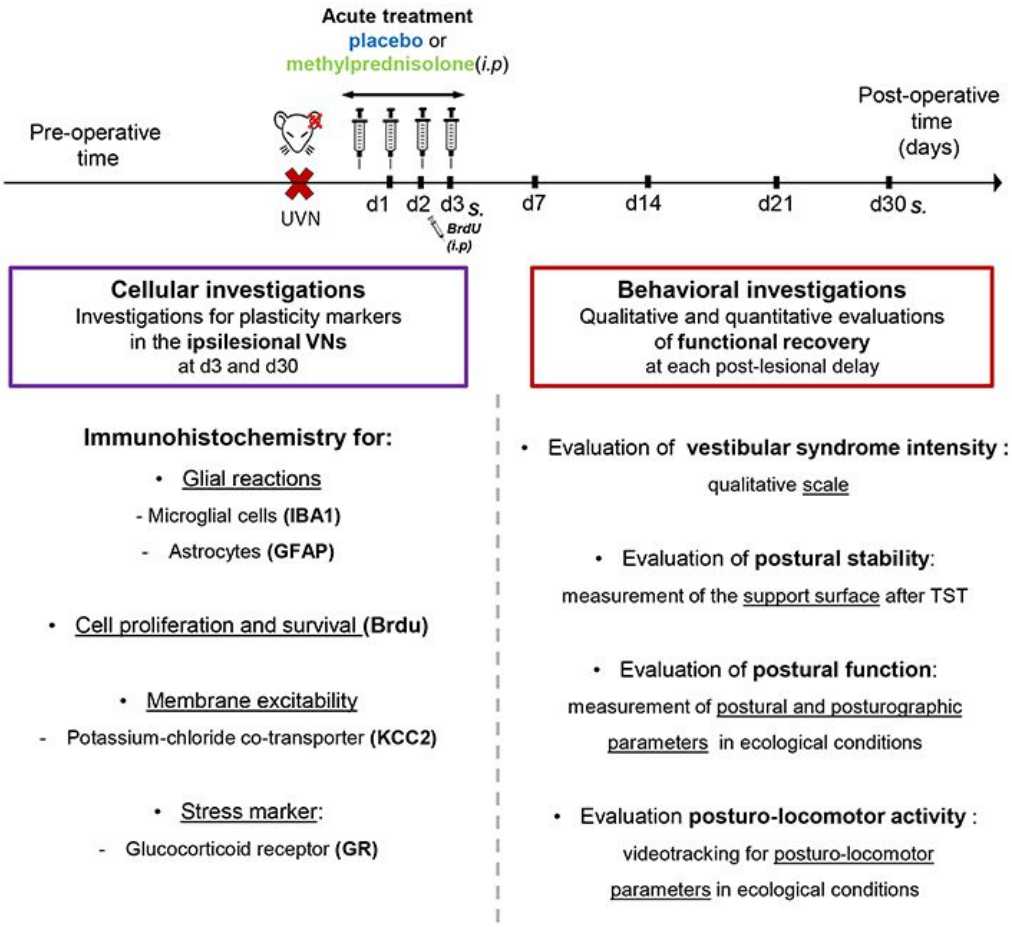

Figure 2

Study design Experimental protocol to study and visualize the impact of the pharmacological blockage of the acute neuroinflammation after UVN on the expression of the plasticity mechanisms observed in the

deafferented VN, as well as on the kinetics on functional recovery in the adult rat. S.: sacrifice i.p: intraperitoneal injections TST: Tail Suspension Test

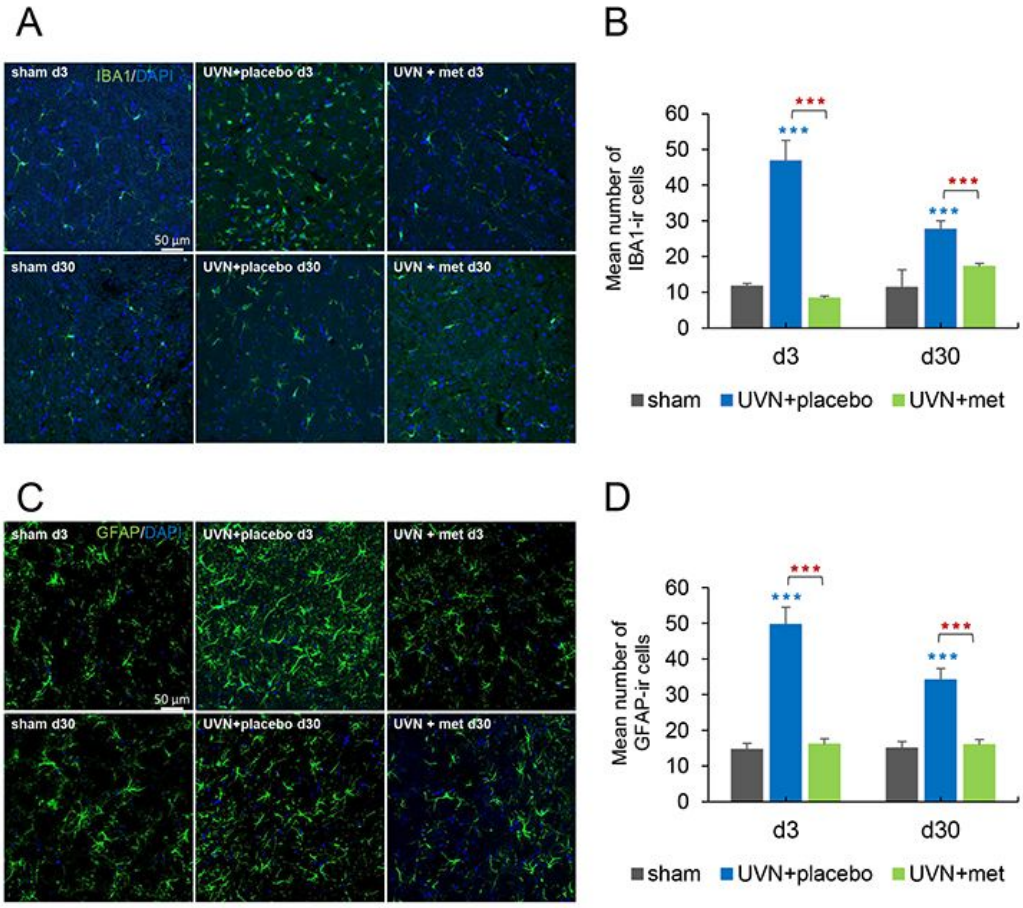

Figure 3

"Please see the Manuscript PDF file for the complete figure caption".

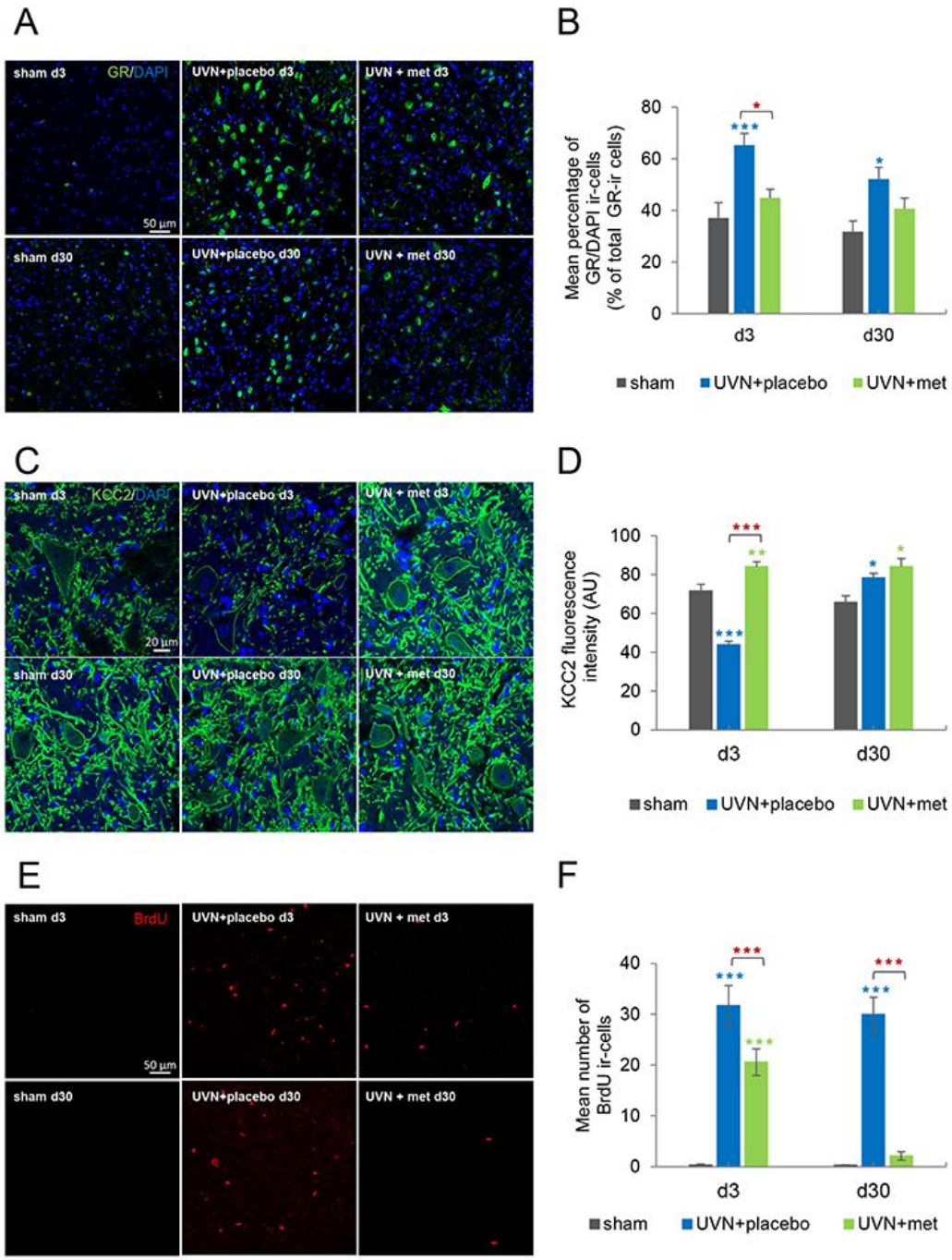

Figure 4

"Please see the Manuscript PDF file for the complete figure caption".

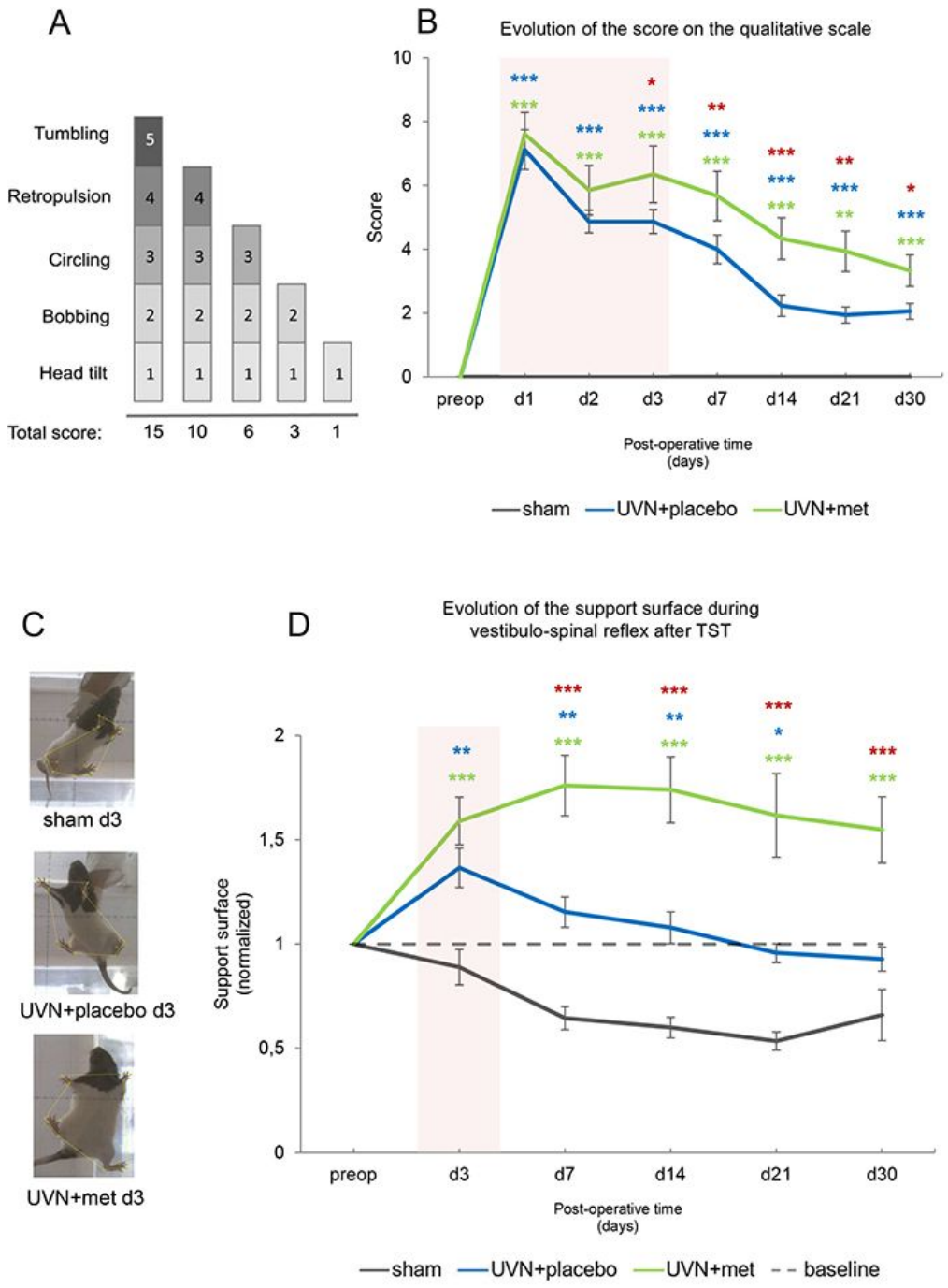

Figure 5

"Please see the Manuscript PDF file for the complete figure caption".

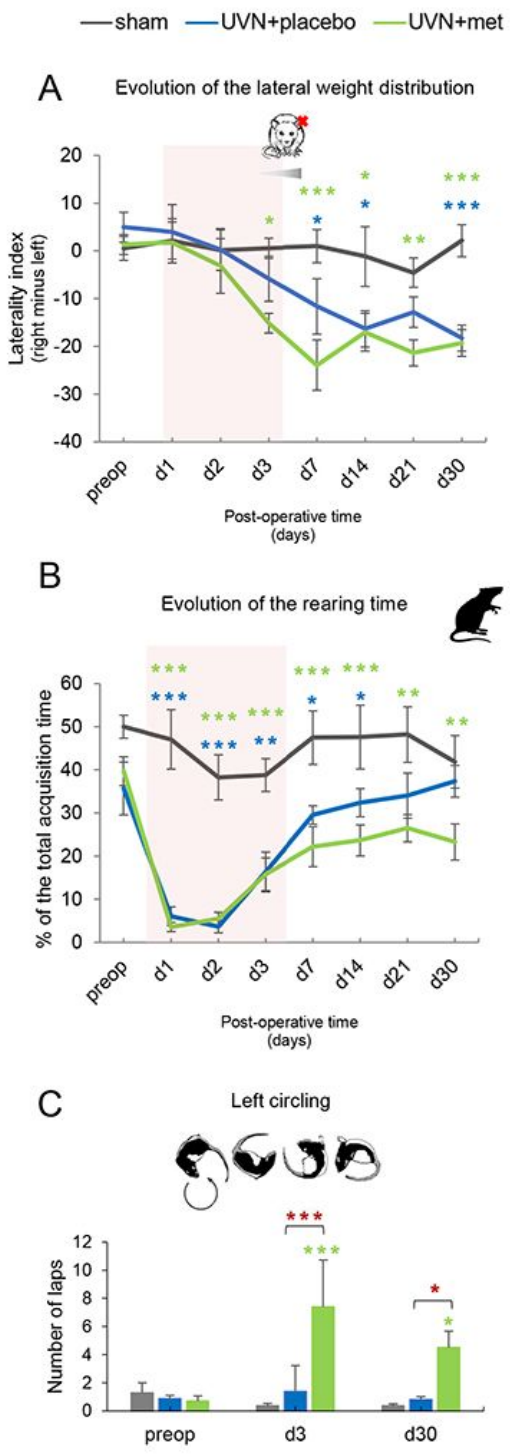

Figure 6

"Please see the Manuscript PDF file for the complete figure caption".

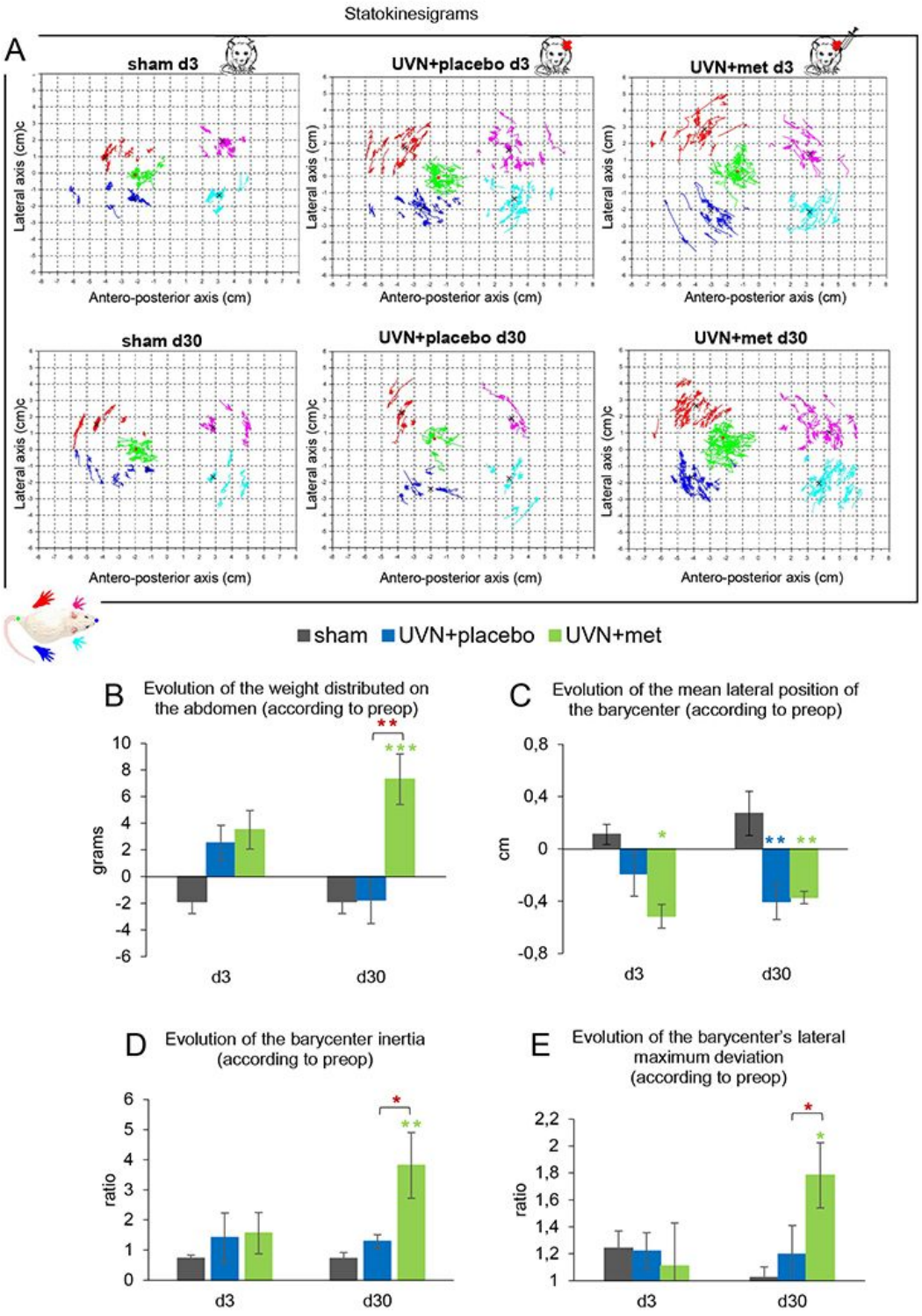

Figure 7

"Please see the Manuscript PDF file for the complete figure caption".

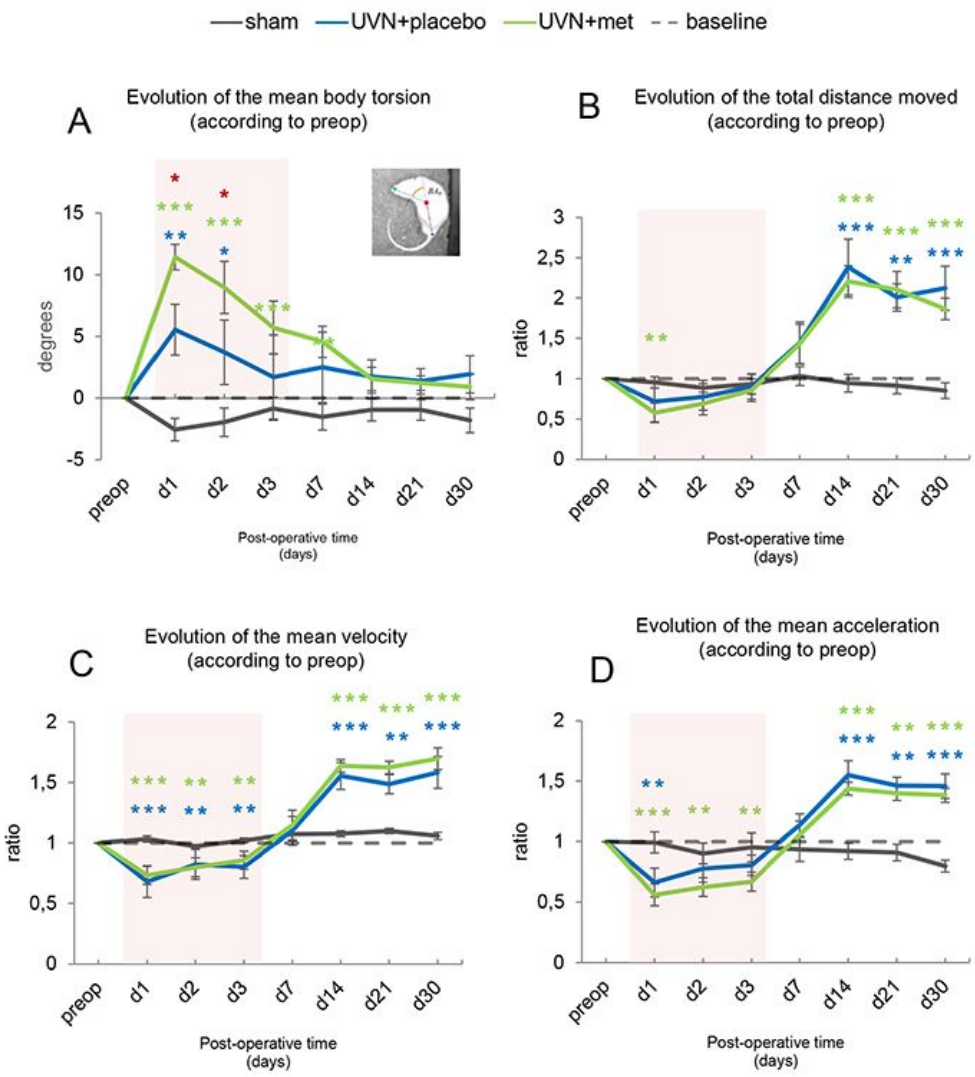

Figure 8

"Please see the Manuscript PDF file for the complete figure caption".